3. Results and Discussion

Present work involves fluorescence studies of doped anthracene luminophors in polycrystalline form. Anthracene belongs to the class of organic molecular solids in which molecules as such are held together by weak van der wall's forces of attraction. Most of the polynuclear aromatic hydrocarbons are molecular solids and are insoluble in water but highly soluble in inert solvents. The dilute solution of molecular solids consists of molecules existing in isolated form whereas in concentrated solution there may be aggregates. The aggregation property is known to depend on the lattice structure of molecular solids.

Characteristics of organic semiconductors are the intermolecular bonds. The alteration of single (σ) and double (π) bonds referred to as conjugation is typical for organic conductors. The carbon atoms involved in this type of bonding are sp2 hybridized. The three hybrid sp2 orbital form the σ bonds with the σ-electrons being highly localized. The remaining non-hybridized Pz orbital of adjacent carbon form the π-orbital perpendicular to σ bonds and delocalized over the molecules. Most of the photophysical properties are because of these delocalized π-electrons. The sigma bonds are very strong and positioned lower in energy. The molecular orbital that are filled (π-bonding orbital) form the valence states. The filled orbital with the highest energy are called the Highest Occupied Molecular orbital (HOMO). The vacant orbital (π^* anti-bonding orbital) form the conduction band, with LUMO being the Lowest Unoccupied Molecular Orbital. Besides this the molecular packing in the solid, determine many physical properties. The intramolecular interaction energy originates from several contributions. The electrostatic interaction between multipoles (usually quadrupoles) and the dispersion forces (van-der wall's) between induced dipoles represents the dominant force. These interactions determine the crystal structure. The molecules may be face to face oriented or may force edge to face stacking. The PAHs are known to be packed into lattice type A, B, AB and lattice D type.

16181

3.1 Anthracene

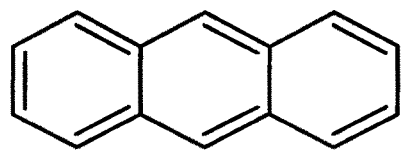

Anthracene crystallizing as lattice 'A' type is reported to be a highly fluorescent as compared to lattice 'A' type molecules are characterized by small π-π orbital overlap between adjacent molecules and hence luminescence in crystalline anthracene is arising from single molecule i.e. monomer fluorescence.

Anthracene is wide band gap semiconducting material and fluoresces in violet region of electromagnetic spectrum. Its spectral characteristics can be changed by traces of impurities or deliberately added dopants [72].

Literature indicates that the anthracene is best solvent in molten state and can solubilize many impurities such as tetracene, pentacene, carbazole perylene etc [73]. Anthracene is widely used in organic electroluminescent diodes and as scintillation material. Its fluorescence is being used to calibrate the fluorescence measuring instrument and also during the determination of quantum efficiency. The visible scintillation spectrum of anthracene is identical with the fluorescence spectrum excited by ultraviolet. The uv-excited anthracene can transfer excitation energies to impurities in it and its fluorescence either quenched or spectrally altered upon interactions occurring between host and impurity molecules. Because of interesting optical and structural properties the anthracene is used as host material in the present studies. With this view to understand the probable molecular interactions between host-guest pair, the optical and structural properties of bare anthracene are studied in the beginning.

3.1.1 Optical properties of anthracene

3.1.1.1 Absorption and Excitation spectroscopy

Fig. 3.1 shows excitation (a) and absorption (b) spectra of anthracene solution without any impurities. Both the spectra show well defined peaks in the uv-region. The spectrum is structured and the peaks appear at 340 nm, 357 nm and 376 nm with a small shoulder in the high energy region. The absorption and excitation spectra are spectrally identical

and band positions are same. This observation indicates that ground state and excited state behavior of anthracene molecules are similar.

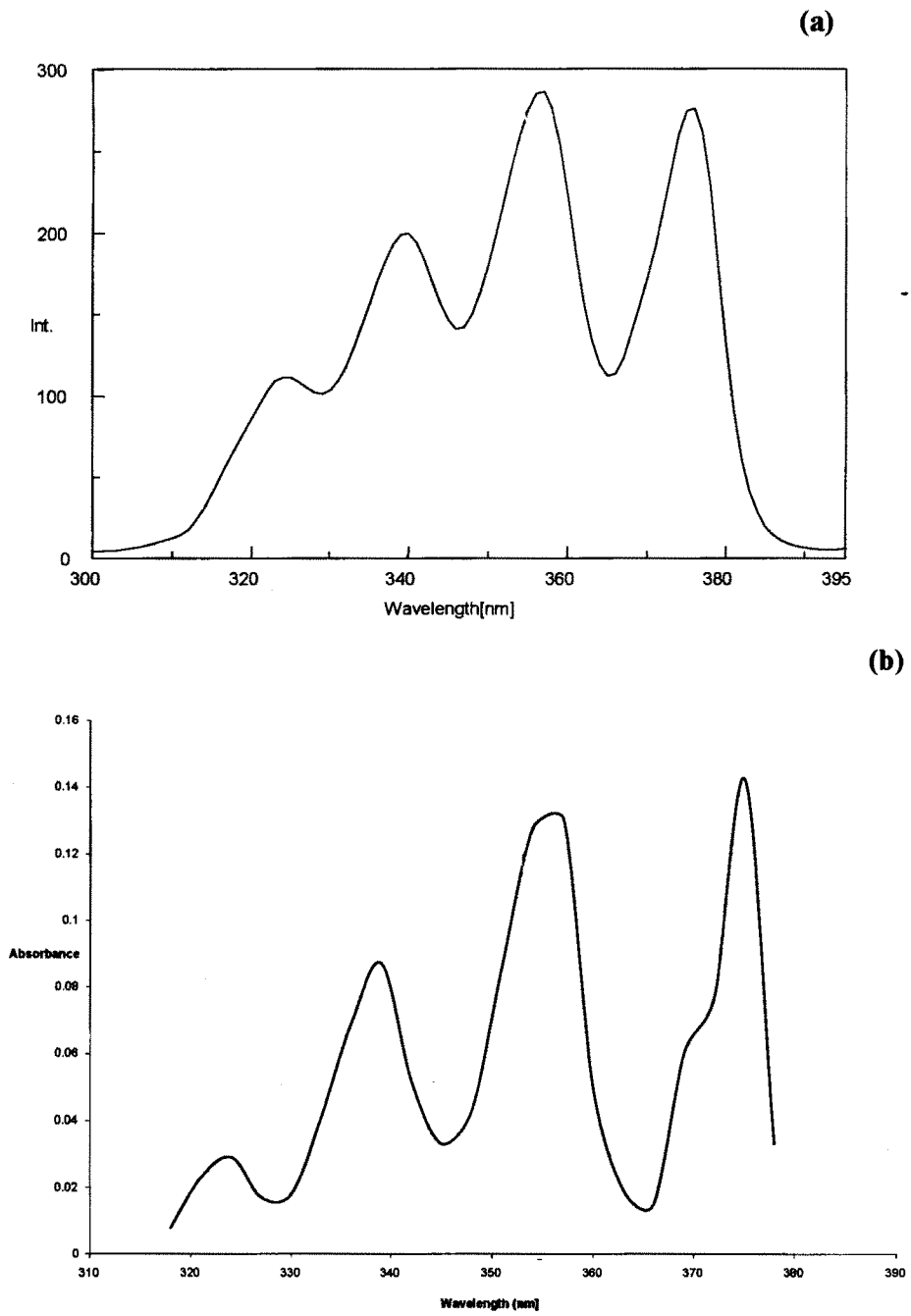

Fig. 3.1 Excitation (a) and absorption (2) spectra of anthracene in solution.

The spectral bands are because of π-π^* transition. The 0→0 band intensity is nearly comparable with 0→1.The fluorescence spectra of anthracene are recorded both in

solution (1) and in crystalline state (2) and presented in Fig. 3.2 along with its excitation spectrum (3). The fluorescence and excitation spectra of anthracene are recorded in solution are sharp and structured and exhibits mirror image relationship with excitation spectrum. The emission bands appear at 378 nm, 401 nm and 423 nm with shoulder at 447 nm. The intense band corresponding to 401 nm gives λ_{max} at 447 nm. The 0←0 emission band at 378 nm overlaps with 0→0 excitation band and hence Stokes shift is negligible as per the expectation. This is additional evidence in support of the purity of anthracene material used in the present studies. The emission band at 401 nm is most intense and determines λ_{max} of anthracene in solution. The fluorescence spectrum of crystalline anthracene shown in same Fig. 3.2 is still structured but exhibit appreciable spectral shift from 0→0 band in excitation spectrum. The emission bands appear at wavelength 427 nm is most intense.

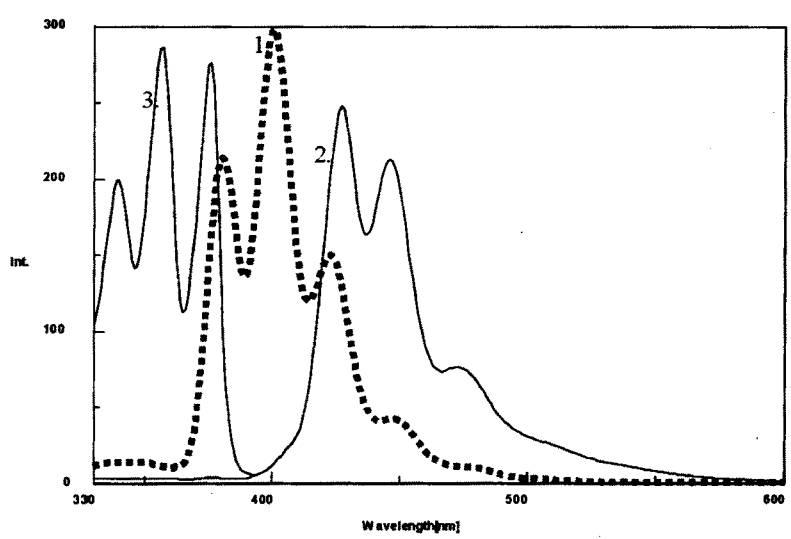

Fig. 3.2 Fluorescence spectra of anthracene in solution (1), in crystalline state (2) and excitation spectrum of anthracene in solution (3).

The fluorescence spectrum of crystalline anthracene is shifted towards red from the spectrum of anthracene in solution. The observed spectral shift between λ_{max} is 1520 cm^{-1}. The large value of spectral shift indicates that emission arising from dilute solution is monomeric in nature and it is a molecular property. However in crystalline state observed

emission is from aggregation. The anthracene crystallizes in lattice 'A' type which is characterized by smaller π-orbital overlap between adjacent molecules. The molecular interactions between adjacent neighboring molecules in crystal decreases the energy of the level from which emission occurs. Hence in crystalline state observed emission is property of crystal as whole and hence referred to as crystal fluorescence. The different polynuclear aromatic hydrocarbons (PAHs) were tested for their optical performance with a view that the doped system in anthracene molecular host could be prepared. The dopant material having electronic structures with first excited singlet energy less than that of anthracene were selected. In addition to this overlap of the absorption spectra of dopant with emission spectrum of anthracene was also examined as larger overlap indicates efficient excitation energy transfer from excited anthracene to dopant molecules. The laborious work in this direction permitted us to used following materials as dopant in anthracene host;

I.] tetracene

II] perylene

III] 9-chloroanthracene and

IV] 9-vinylanthracene

Of these tetracene and perylene are non substituted planer, non polar molecules, whereas 9-chloro, 9-vinyl and 9-methyl anthracene are non-planer substituted polar molecules. The optical performance of these dopants was studied first to understand their effect on structural and emission properties when intentionally incorporated in anthracene lattice by doping technique.

3.2 Tetracene

Planer molecule with four benzene rings linearly condensed.

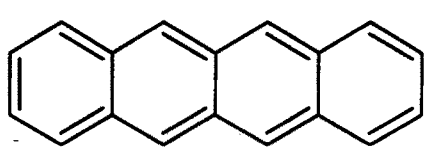

3.2.1 Structural properties

It is four-ring analogue in the naphthalene, anthracene series of linear, fused benzene rings. The X-ray diffraction studies revealed triclinic structure of tetracene with two

molecules per unit cell [74, 75]. Tetracene is known to form excellent solid solution over a wide range of concentrations with monoclinic PAHs inspite of their difference in crystal structure [76]. Many other analytical techniques such as electron and X-ray diffraction, fluorescence resonance in magnetic field, optical spectroscopy have been reported in literature which has investigated bulk structure of tetracene.

3.2.2 Optical properties

The fluorescence (1) and excitation (2) spectra of tetracene solution are presented in Fig.3.3. Both the spectra exhibit exact mirror image relationship with very smaller separations of 260 cm^{-1} in 0→0 band of excitation and 0→0 band in fluorescence spectrum. The maximum in the excitation is at 477 nm while in fluorescence spectrum it is 483 nm and corresponds to green color. The structured, sharp fluorescence spectrum indicates that like anthracene tetracene is also exhibit monomeric emission from its solution. The emission spectrum of anthracene and excitation spectrum of tetracene exhibits very large overlap. This is the reason because of which anthracene doped by tetracene is treated as classic system where very efficient transfer of singlet energy occurs. The crystalline tetracene neither exhibited absorption nor fluorescence spectra.

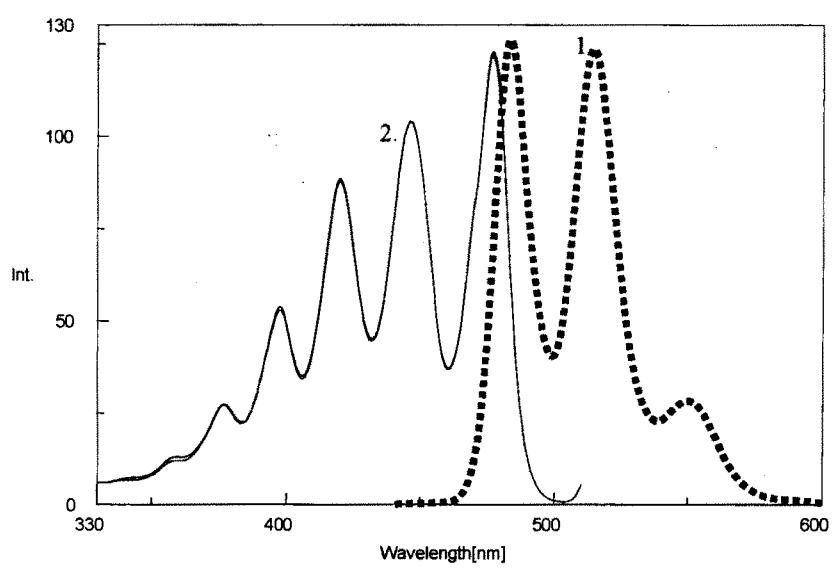

Fig. 3.3 Fluorescence (1) and excitation (2) spectra of tetracene in solution.

Fig. 3.4 shows excitation (a) and absorption (b) spectra of tetracene in solution. The absorption and excitation spectra are banded and identical [77]. The bands in excitation spectrum are well defined and appear at 477 nm, 450 nm, 425 nm, 397 nm and 375 nm. The absorption spectrum is rather weaker and exhibits bands at 440 nm, 410 nm and 380 nm.

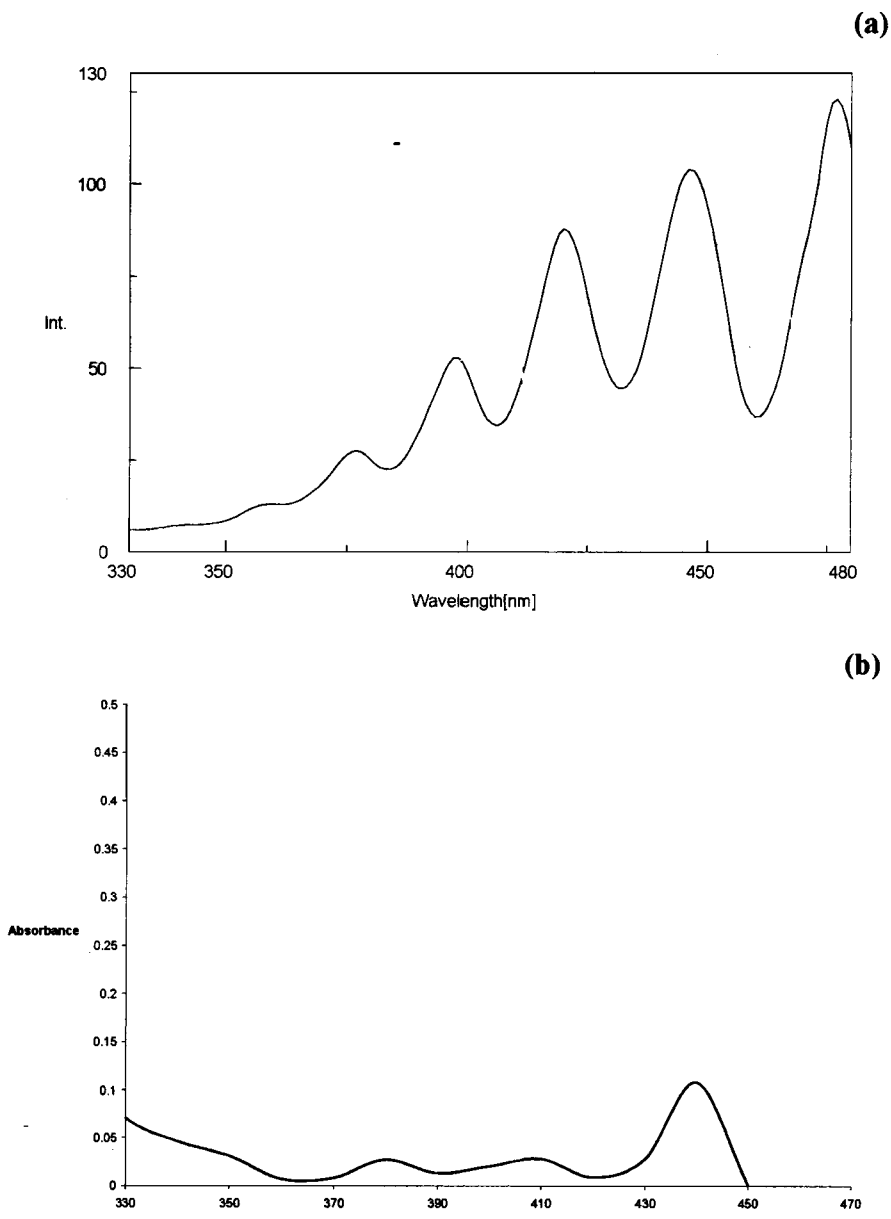

Fig. 3.4 Excitation (a) and absorption (b) spectra of tetracene in solution.

The nature of both spectra indicates that in the ground and excited state tetracene exists as single molecule.

3.3 Perylene

It is polycyclic aromatic hydrocarbon with molecular formula $C_{20}H_{12}$. Five benzene rings are cross linked in its structure.

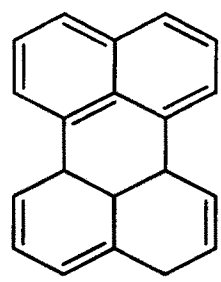

3.3.1 Structural properties

It is soluble in most of organic solvents and ambient light is enough to see its blue fluorescence in solution. Perylene molecules are widely used as fluorescence probe in different research fields since it forms characteristic excimer in excited state. High fluorescence quantum yield, photostability, thermal stability and efficient carrier mobility also make perylene an excellent candidate as organic semiconductor as well as organic electroluminescent material. Owing to highly hydrophobic property and red color emission of excimer, perylene molecules have been used in several biological investigations as well as DNA detection and probing of physical status of membrane. The perylene crystallizes in lattice 'D' type and lateral π-orbital overlap between adjacent molecules is larger and excimer formation is favored.

3.3.2 Optical properties

The absorption spectrum of perylene is shown in Fig. 3.5 (b). The spectrum is structured and absorption bands appear at 410 nm and 438 nm. The maximum absorption is at 438 nm. The excitation spectrum shown in same Fig. 3.5 (a) is also structured and matches well with the absorption spectrum. The excitation bands are at 433 nm, 410 nm and 380 nm with maximum at 433 nm.

(a)

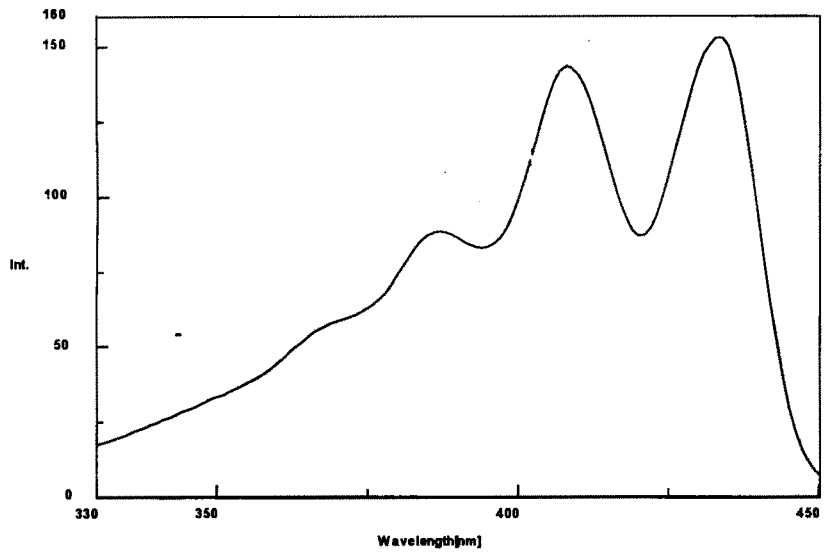

(b)

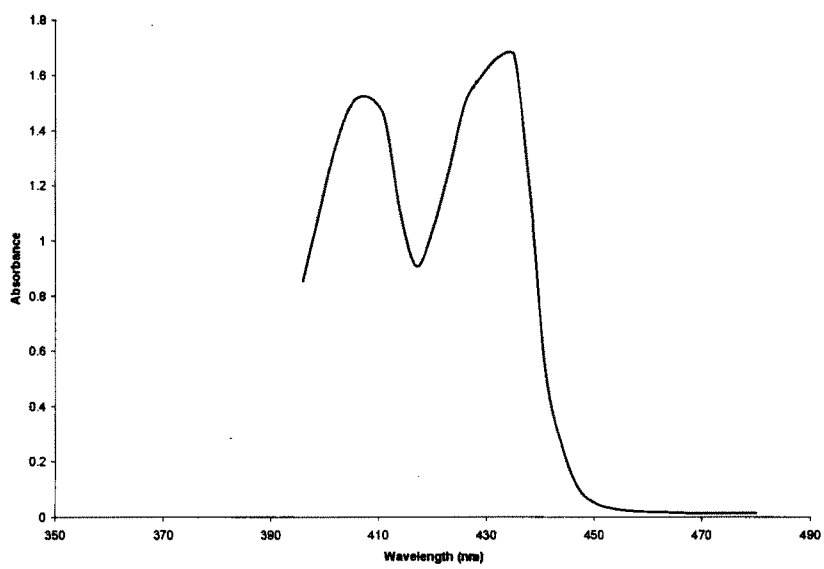

Fig. 3.5 Excitation (a) and absorption (b) spectra of perylene in solution.

The fluorescence spectrum of solution of perylene shown in the Fig.3.6 (1) is structured and exhibit mirror image relationship with excitation spectrum with small Stokes shift of about 420 cm^{-1}. The dilute solution spectrum of perylene exhibits monomeric fluorescence. The fluorescence spectrum of crystalline perylene shown in

Fig.3.6 (2) is broad, structure less band with maximum at about 563 nm. This spectrum is attributed to well known excimer emission of perylene as its 'D' type lattice structure favors aggregates due to lateral π-orbital overlapping. The excimer emission band shows pronounced red shift of 5330 cm^{-1} from monomer emission band. The absorption in blue region of visible spectrum led this molecule to act as an acceptor in anthracene and similar molecules emitting in blue region

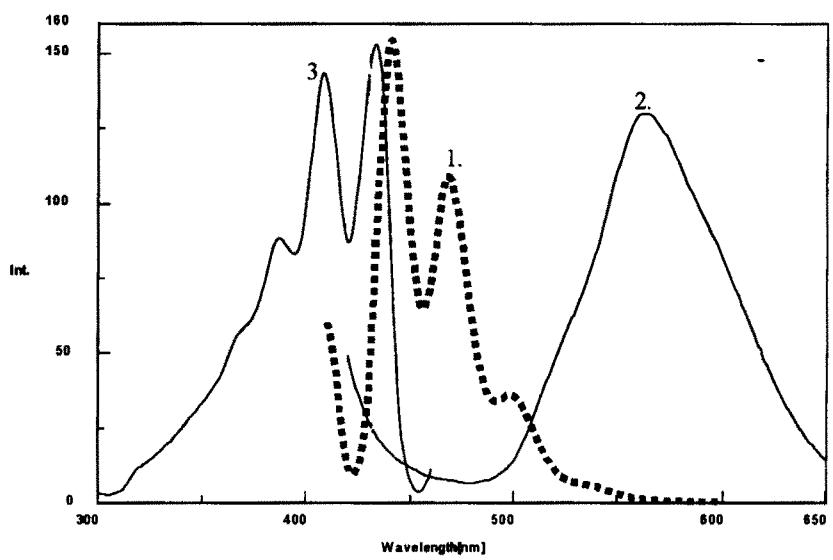

Fig. 3.6 Fluorescence spectra of perylene in solution (1), in crystalline state (2) and excitation spectrum of perylene in solution (3).

3.4 9-Vinylanthracene (VA)

It is regarded as 9-substituted anthracene derivative.

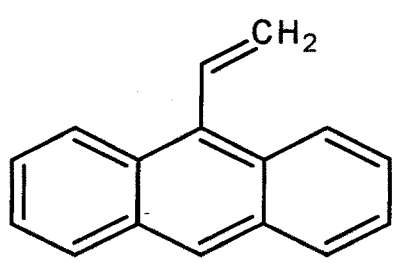

3.4.1 Structural properties

It is efficient fluorescent compound having high quantum yield 0.91. It is shown that this 9-substituted anthracene undergo photodimerization rather than typical vinyl aryl

photopolymerization. VA is used as high grade primary and secondary scintillators capable of replacing widely used 1,4-bis-(2-(5-phenyl)-oxazolyl)-benzene (POPOP). Vinyl substitution makes VA more polar.

3.4.2 Optical properties

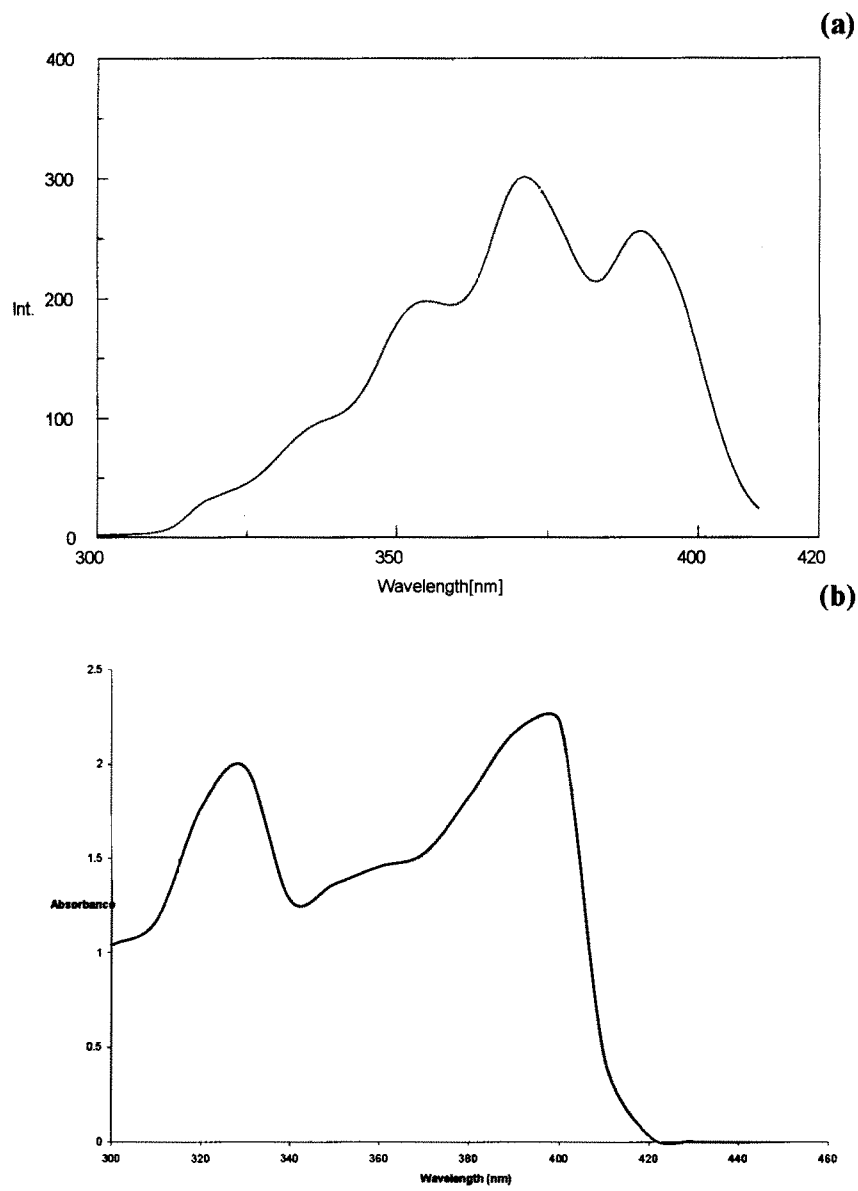

Fig. 3.7 Excitation (a) and absorption (b) spectra of 9- vinylanthracene in solution.

Fig. 3.7 shows absorption (a) and excitation (b) spectra of dilute solution of VA. Both the spectra are structured appear in same spectral region. The wavelength of maximum

obtained from excitation spectrum is 371 nm while in absorption spectrum it is 400 nm. The spectrum of VA is not as sharp as anthracene. It is concluded that vinyl group at 9-position on anthracene ring restricts vibrational transition. In addition larger π-orbital overlap between two adjacent molecules increases molecular interactions. Hence absorption and excitation spectra of VA are red shifted when compared with the spectral region of anthracene Fig. 3.1.

3.5 9-Chloroanthracene (CA)

It is also regarded as 9-substituted anthracene derivative.

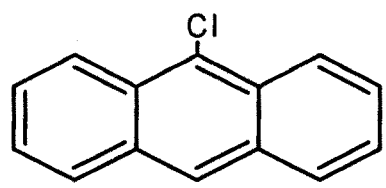

Fig. 3.8 shows fluorescence spectra of crystalline CA (2), dilute solution of CA (1) and its excitation spectrum (3).

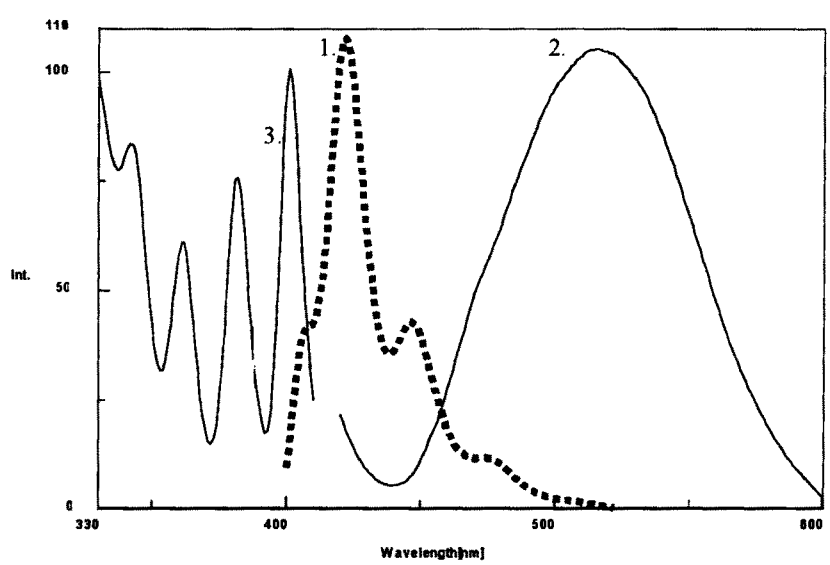

Fig. 3.8 Fluorescence spectra of 9-chloroanthracene in solution (1)and in crystalline state (2) and excitation spectrum of 9-chloroanthracene in solution (3).

Though the excitation spectrum of dilute solution of CA is structured with sharp bands like the anthracene in solution, it is spectrally shifted towards red. The 0→0 band

in anthracene spectrum appears at 376 nm while that in CA at 401 nm. The emission spectrum is also red shifted. The 0←0 emission band in anthracene spectrum is observed at 378 nm while in CA appears at 422nm. The observed Stokes shift is 5550 cm^{-1}. The larger Stokes shift indicates that the electron donating chloro group shifts emission to red and exhibit bathochromic effect. It is concluded that the chlorosubstitution tends to decrease the energy of excited level from which emission occurs. In addition to the chlorosubstituted anthracene favor lateral π-orbital overlap between adjacent neighboring molecules and hence crystal emission is a structureless broad band peaking at 516 nm. The spectral shift in solution and crystal emission band is at 4550 cm^{-1}. The larger spectral shift indicates that the CA belongs to lattice 'D' type crystal where neighboring molecules favor lateral π-orbital overlapping.

3.6 Structural and photophysical Properties of doped anthracene Luminophors

3.6.1 Perylene doped anthracene luminophors

Anthracene was doped by various amounts of perylne.The crystalline anthracene is bluish white in color while perylene is orange. A small addition of perylene drastically changes the color of anthracene from blue to violet. The visual color seems to become dark with addition of perylene. The observed color change indicates incorporation of perylene molecules in lattice of anthracene. The crystalline doped luminophors were finely ground and tested for homogeneity by X-ray diffraction spectroscopy.

3.6.1.1 Structural features

X-ray Diffraction Studies

Anthracene and perylene form series of solid solutions. The X-ray Diffraction Profile (XRD) of doped and pure anthracene presented in Fig.3.9 shows sharp and well defined peaks indicating crystalline behavior of the luminophors. The XRD pattern of pure anthracene (A) is used as a fingerprint with which spectra of doped anthracene are compared. It is observed that the position of the peaks (2θ values) change very slightly. No additional peaks are seen in XRD profile of doped samples which is an indication of formation of homogeneous mixed crystals. The prominent lines on the XRD pattern were indexed on the basis of monoclinic unit cells, the value of lattice constants being a = $8.54A^{O}$, b = $6.00A^{O}$, C = $9.45A^{O}$ and $\alpha = \gamma = 90^{0}$ and $\beta = 103.4^{O}$ [11]. The intense band

[001] was used to calculate grain size of doped anthracene by using Scherer formula [71]. The calculated values of grain size are presented in Table No. 5. An examination of these values reveals that the grain size of anthracene decreases with increase in concentration of perylene. The decrease of grain size may be attributed to the formation of newer smaller grains over the larger grains. Doping of a pure crystal by intentional addition of impurity creates defects and imperfection and the host crystal is deformed. It is expected that nearly all crystals in nature grown at supersaturation will contain dislocation as otherwise they could have grown. The deformation in the crystal changes microstain ($\mathcal{E}$) and dislocation density (ρ) which were calculated by using following relation [78].

$$\varepsilon = \frac{\beta_{2\theta}\cos\theta}{4} \qquad \text{----------} \qquad (1)$$

$$\rho = \frac{15\varepsilon}{aD} \qquad \text{----------} \qquad (2)$$

$$t = \frac{0.9\lambda}{Dp\cos\theta} \qquad \text{----------} \qquad (3)$$

where, '$\beta_{2\theta}$' and 'Dp' is the full width at half maximum, 'λ' the wavelength of CuKα radiation (1.54 x 10^{-10} m), 'a', the lattice constant, 'D', the grain size and '$\mathcal{E}$' is microstain.

The values of $\mathcal{E}$ and ρ, tabulated in Table No. 5 seen to increase slightly with increase in concentration of perylene in anthracene which is as per the expectation. During the mixed crystal growth partial displacement of anthracene molecules from their sites by perylene or interstitial substitution upset the regular molecular sequence in the lattice to produce a stacking fault. The result is then the mixture of two molecules in the doped lattice. The stacking fault is calculated by using the relation,

$$\alpha_{st} = \left[\frac{2\pi^2}{45(3\tan\theta_{001})^{1/2}}\right]\beta \qquad \text{----------} \qquad (4)$$

The value of α_{st} given in same Table No. 5 increases with increase in perylene concentration. This result led us to consider the closely packed structure of anthracene and perylene in mixed crystals.

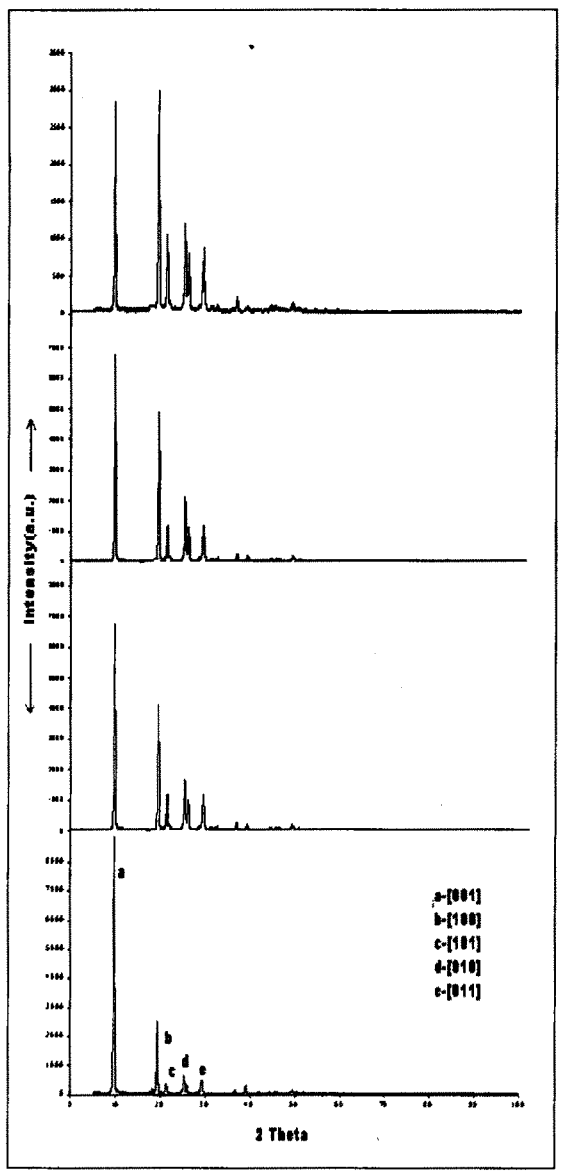

Fig.3.9 Powder X-ray diffraction profile of anthracene and perylene doped anthracene. A) Pure anthracene B) $2x10^{-2}$, C) $3x10^{-2}$ and D) $5x10^{-2}$ mole of perylene per mole anthracene.

Table No. 5:- Structural parameters of perylene doped anthracene luminophors.

Concentration Moles of perylene per mole anthracene	Glancing angle (2θ) degree	FWHM $\beta_{2\theta}$	Microstain $\varepsilon \times 10^{-3}$ l^2/m^{-4}	Dislocation density $\rho \times 10^{15} cm^{-2}$	Grain size (D) A^O	Stacking fault α_{st}
0	9.702	0.345	1.71	1.51	201.4	0.2995
2×10^{-2}	9.580	0.355	1.76	1.58	195.7	0.3103
3×10^{-2}	9.259	0.410	2.04	2.09	170.9	0.3645
5×10^{-2}	9.636	0.431	2.14	2.33	161.2	0.3750
1×10^{-1}	9.414	0.451	2.24	2.56	154.0	0.3970

3.6.1.2 Fluorescence of perylene doped anthracene mixed crystals

The fluorescence spectrum of crystalline anthracene (1), crystalline perylene (3) and perylene doped anthracene (2) are presented in Fig. 3.10. It is seen that addition of small amount of perylene quenches the intensity of emission bands of anthracene at 427 nm and 446 nm and new structureless, broad emission band appear in the region 450 nm to 600 nm. This band does not match with the orange excimer emission band appearing in the region 490 nm to 700 nm with maximum at 563 nm [79]. The monomer emission of perylene expected to occur in the range 425-500 nm is not seen in the fluorescence spectrum of doped anthracene [34].

In the most of mixed crystals addition of small mole fraction of dopant to anthracene quenches the anthracene fluorescence and yields intense fluorescence characteristics of dopant [21]. This shows that there is efficient transfer of electronic excitation energy from host to dopant molecule. The fluorescence of host is almost quenched and that of dopant appears. However in the present system though the fluorescence of anthracene is quenched by perylene, its characteristics emission is not observed in the fluorescence spectrum of mixed crystal. The broad fluorescence is attributed to exciplex type fluorescence [80]. The UV-Excitation may induce the formation of anthracene-perylene overlapped structure in doped system.

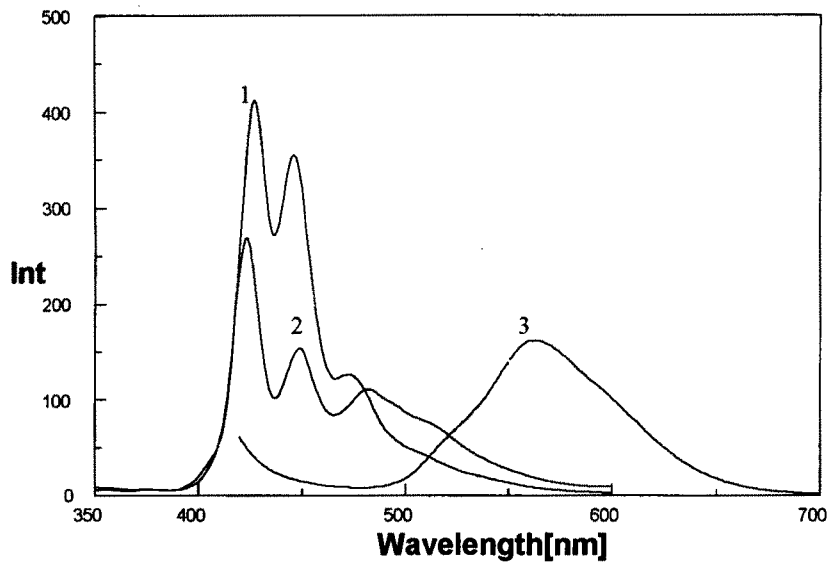

Fig. 3.10 Fluorescence spectra of crystalline anthracene (1), perylene doped anthracene (2) and crystalline perylene (3).

To examine the possibility of exciplex formation, the series of doped anthracene crystalline powders containing varying amounts of perylene were prepared and their fluorescence spectra were recorded at an excitation wavelength corresponding to anthracene excitation energy. The fluorescence spectra of anthracene luminophors containing varying amounts of perylene are displayed in Fig. 3.11. Careful observation of figure reveals that the fluorescence of anthracene is quenched gradually by successive addition of perylene dopant. The smaller addition of perylene quenches the anthracene fluorescence but the broad exciplex emission band was not seen. The perylene monomer expected to occur with bands at 416 nm, 446 nm and 473 nm at lower concentration are not seen clearly. Some of the emission bands of perylene seem to be masked in the anthracene fluorescence. Exciplex emission band with maximum at 500 nm is seen only at higher concentration i.e. above 2 x 10^{-2} mole concentration of perylene per mole anthracene. At still higher concentration the red broad band gets broadened. The excimer emission of perylene with maximum at 563 nm is not seen even at higher concentration of perylene in anthracene.

BARR. BALASAHEB KHARDEKAR LIBRARY
SHIVAJI UNIVERSITY, KOLHAPUR.

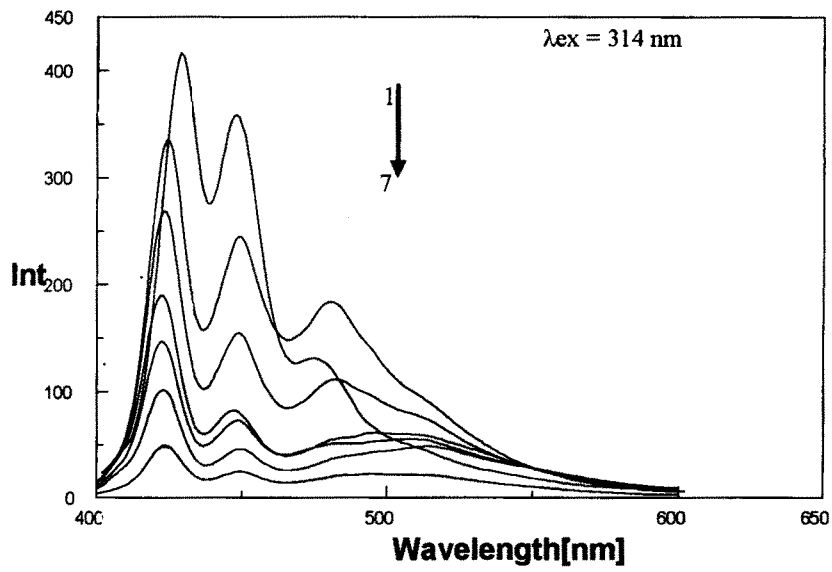

Fig.3.11 Fluorescence spectra of anthracene luminophors containing varying amounts of Perylene: (1) 0 mole of Perylene, (2) $5x10^{-3}$, (3) $1x10^{-2}$, (4) $2x10^{-2}$, (5) $3x10^{-2}$, (6) $5x10^{-2}$, and (7) $1x10^{-1}$ mole perylene anthracene.

The spectral parameters of anthracene luminophors obtained from fig. are given in Table No. 6. The table shows monomer anthracene fluorescence wavelength (λ_M) with its intensity F_M, exciplex emission wavelength (λ_E) with its intensity F_E and ratio of intensity of exciplex to monomer emission. From the table it is seen that monomer fluorescence intensity decreases continuously with perylene concentration. The ratio F_E/F_M also increases and seems to saturate at higher perylene concentration. The presence of lower amount of perylene in anthracene quenches the fluorescence of anthracene due to excitation energy transfer or charge transfer between them. The charge transfer is favored only in higher concentration of dopant. It is also a diffusional process and favored in solution containing donor-acceptor pair. Hence initially the quenching is because of EET. It is also known that singlet energy of perylene is lower lying than that of anthracene which indicates the possibility of energy transfer [81]. The probable energy level diagram constructed from emission wavelength of singlet fluorescence shown in Fig. 3.12 suggests possibility of singlet-singlet energy transfer from anthracene to perylene.

Table No.6:- Spectral parameters of perylene doped anthracene luminophors.

Sr. No.	Concentration of Perylene per mole f Anthracene	Monomer fluorescence		Exciplex fluorescence		F_E/F_M
		λ_M	F_M	λ_E	F_E	
1	0	425	410	-	-	-
2	$5x10^{-3}$	425	340	-	-	-
3	$1x10^{-2}$	425	270	-	-	-
4	$2x10^{-2}$	425	195	500	70	0.3589
5	$3x10^{-2}$	425	145	500	60	0.4137
6	$5x10^{-2}$	425	100	500	50	0.5000
7	$1x10^{-1}$	425	50	500	25	0.5000

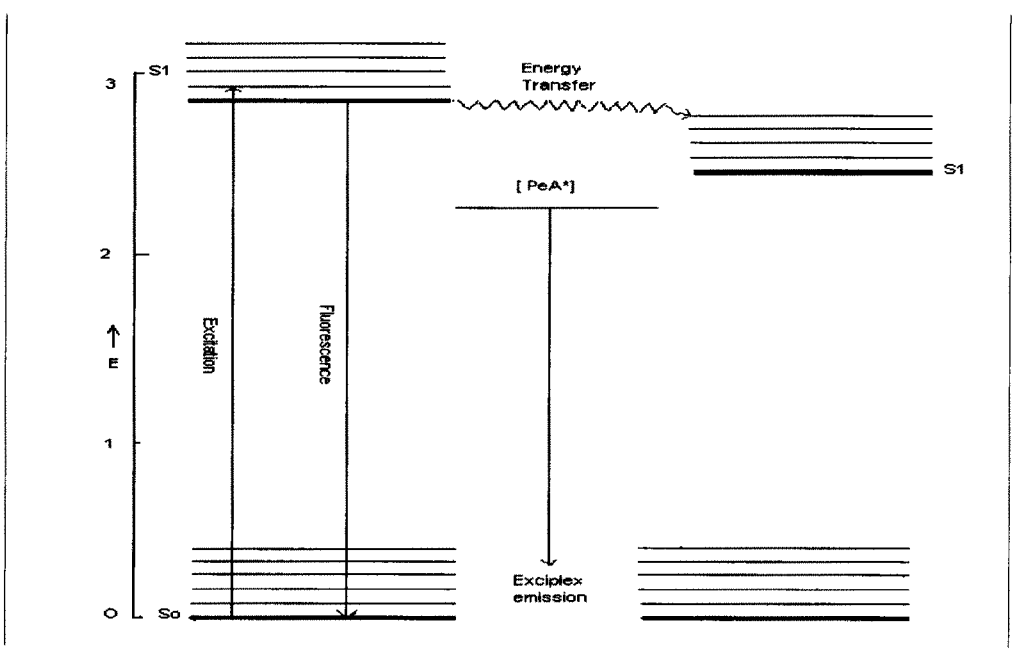

Fig. 3.12 Energy level diagram.

The efficient energy transfer between host and dopant molecule is examined by overlap between emission spectrum of host and absorption spectrum of dopant. Fig. 3.13 shows region of overlap between fluorescence spectrum of crystalline anthracene (1) and

absorption spectrum of perylene in solution (2). The shaded region of overlap shows larger overlap between two spectra and indicates efficient energy transfer between anthracene and perylene. Hence though perylene monomer fluorescence is not observed the anthracene fluorescence quenching is because of transfer of energy from anthracene to perylene. As the amount of perylene increases the quenching also increases.

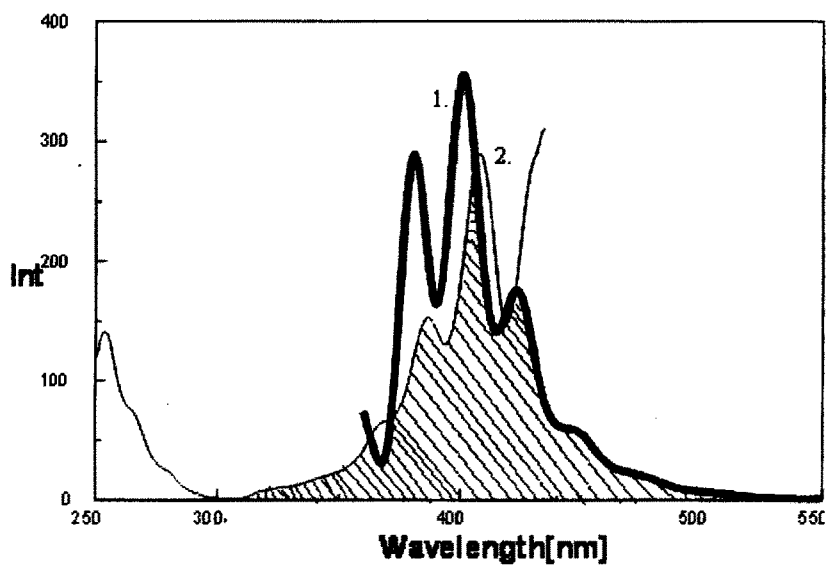

Fig.3.13 Region of overlap between fluorescence spectrum of anthracene (1) and absorption spectrum of perylene (2).

The probability of excitation energy transfer is also examined by determining the critical energy transfer distance (Ro) using Forster relation [18].

$$Ro^6 = \frac{9000 \times K^2 \times \Phi_D \times \ln 10}{128 \times \Pi^5 \times n^4 \times N_A} \int \frac{F(\nu)\varepsilon(\nu)\partial\nu^-}{\nu^4} \quad \text{----------} \quad (5)$$

K^2 - orientation factor (0.444)

ϕ_D - Fluorescence quantum efficiency of donor (Anthracene) (0.7).

n - Refractive index of materials of solids n =1

N_A - Avogadro's number (6.023 x 10^{23})

$\int \frac{F(\nu)\varepsilon(\nu)\partial\nu^-}{\nu^4}$ - integrated overlap area.

$$Ro^6 = 3.8353 \times 10^{-7}\ cm$$

$$Ro = 38.3\ A^o$$

The region of overlap between emission spectrum of anthracene and absorption (excitation) spectrum of perylene was used to estimate the value of integral overlap area. The value of Ro less than 50A° indicates efficient energy transfer between host and guest molecules [19].

The higher amount of perylene in anthracene introduces one more additional change in the spectrum as broad structureless tail towards red. This structureless spectrum becomes broader at higher concentration with slight shift in wavelength of maximum emission. The structureless, broad band is attributed to exciplex of perylene and anthracene. At higher concentration perylene excimer is expected but observed emission does not correspond with excimer emission of perylene. Therefore, broad red shifted band is arising due to exciplex formation and its subsequent dissociation gives characteristics exciplex emission as is seen in Fig. 3.11.

Following mechanism is proposed for fluorescence quenching and exciplex formation:

Presentation	**Process**	**Rate**
1. $A_{So} + h\upsilon$ — $[A_{S1}]^*$	Anthracene excitation	Ia
2. $[A_{S1}]^*$— $A_{So} + h\upsilon_f$	Anthracene fluorescence	$k_f [A_{S1}]^*$
3. $[A_{S1}]^*$— $A_{So} + \Delta$	Internal conversion	$k_{IC} [A_{S1}]^*$
4. $[A_{S1}]^*$ — $A_{So} + \Delta$	Intersystem crossing	$k_{ISC} [A_{S1}]^*$
5. $[A_{S1}]^* + Pe_{So}$— $A_{So} + [Pe_{S1}]^*$	EET	$k_{et} [A_{S1}]^* [Pe_{So}]$
6. $A_{So} + [Pe_{S1}]^*$ — $[PeA]^*$	Exciplex formation	$k_{ex} [A_{So}] [Pe_{S1}]^*$
7. $[PeA]^*$ — $Pe_{So} + A_{So} + h\upsilon_{ex}$	Exciplex emission	$k_{-ex} [PeA]^*$

Using our terminology and the kinetic scheme proposed above the equation for relative quantum efficiency of anthracene fluorescence in presence and absence of

perylene are derived. The steady state equation for the transient singlet excited anthracene species $[A_{S1}]^*$ gives following equations,

$$\Phi_f^o = \frac{k_f[A_{S1}]^*}{Ia} = \frac{k_f + k_{ic} + k_{isc}}{Ia}\frac{Ia}{k_f} \quad \text{----------} \quad (6)$$

$$\Phi_f^o = \frac{k_f + k_{ic} + k_{isc}}{k_f} \quad \text{----------} \quad (7)$$

$$\Phi_f = \frac{k_f}{k_f + k_{isc} - k_{ic} + k_{et}[Pe_{So}]} \quad \text{----------} \quad (8)$$

$$\frac{\Phi_f^o}{\Phi_f} = 1 + \frac{k_{et}}{k_f + k_{isc} + k_{ic}}[Pe_{So}] \quad \text{----------} \quad (9)$$

$$\frac{\Phi_f^o}{\Phi_f} = 1 + \frac{k_{et}}{k_f + \sum Ki}[Pe_{So}] \quad \text{----------} \quad (10)$$

Where, ϕ_f^o and ϕ_f are quantum efficiencies in absence and in presence of perylene.

The quantum efficiencies can be expressed in terms of the fluorescence intensities for relative ratio,

$$\frac{F^o}{F} = 1 + \tau.k_{et}[Pe_{So}] \quad \text{----------} \quad (11)$$

The expression is of the Stern-Volmer type. The straight line nature and intercept indicates validity of the equation. The value of rate constant of energy transfer was estimated from the slope of plot and life time of anthracene without perylene. The estimated value of rate constant of energy transfer is of the order of 2.4779×10^{11} and is of higher order than the excitation energy transfer rates estimated for donor-acceptor system in solution which is of the order of 1×10^{-9} sec [82]. It is believed that in mixed crystal the perylene molecule form stacked structure within anthracene lattice reducing the intermolecular distance between them. This explains the higher rates of energy transfer in doped anthracene. Experiments are also performed to examine excitation energy transfer and exciplex formation between anthracene and perylene in solution.

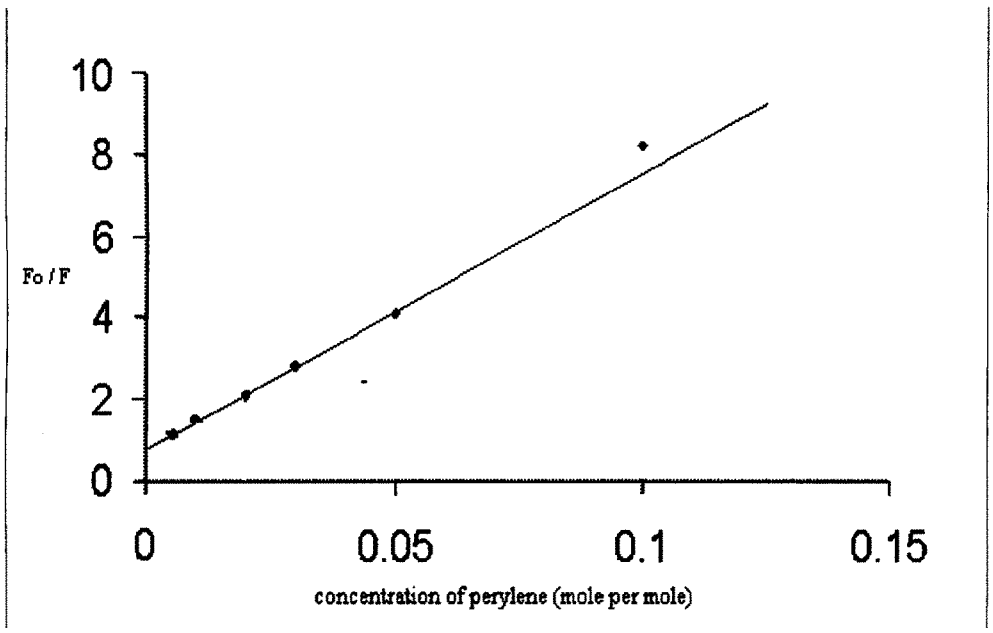

Fig. 3.14 Stern- Volmer Plot.

Fig. 3.15 shows fluorescence spectra of anthracene solution recorded in presence of higher amounts of perylene in n-hexane. The fluorescence of anthracene is quenched and that of perylene monomer appears. The successive additions of perylene quench anthracene fluorescence gradually and that of monomer perylene fluorescence is enhanced. The broad emission band of monomer expected to occur in the region 450-600 nm is not seen even at higher concentration of perylene. The wider distance of separation in solution between anthracene and perylene does not favor exciplex formation and emission. Hence exciplex formation is possible only in polycrystalline anthracene doped by higher amounts of perylene.

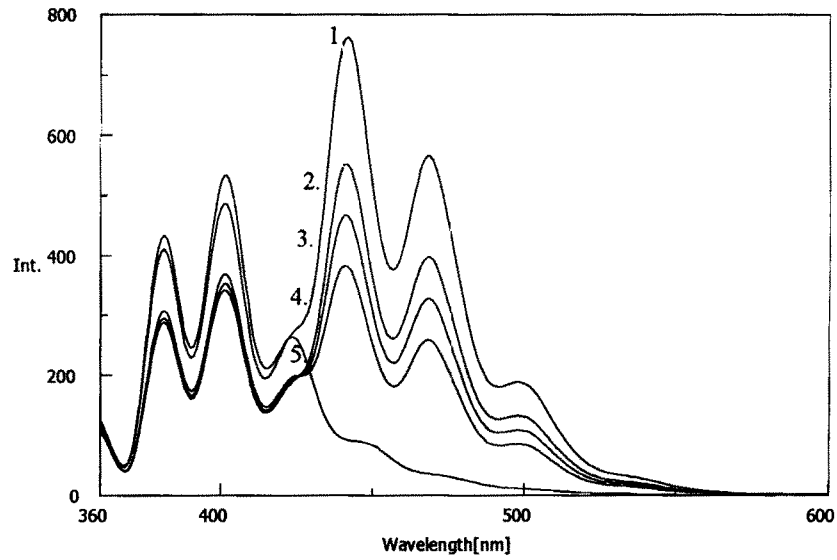

Fig.3.15 Fluorescence spectra of anthracene in solution (1) containing varying amounts of perylene; 2) $3x10^{-6}$M, 3) $4X10^{-6}$ M, 4) $5x10^{-6}$ M and 5) $7X10^{-6}$M.

3.6.2 Tetracene Doped Anthracene Luminophors

The anthracene doped by tetracene crystalline luminophors is a classical system where efficient transfer of energy from donor to acceptor molecule takes place. The possibility of energy transfer is because of selective excitation of donor, at which acceptor molecules are not at all excited. Hence it is a system involving true excitation energy transfer.

3.6.2.1 Optical properties

The crystalline tetracene does not exhibit extrinsic fluorescence when exposed to radiation corresponding to its excitation energy. However solution of tetracene in an inert solvent hexane fluoresce very weakly with green emission (λ_{ex} = 483 nm). Therefore the way to observe intense green color of tetracene is to incorporate it into anthracene crystals by doping and make EET process more efficient by optimizing parameters influencing tetracene emission. With this view the tetracene doped anthracene crystalline powders were prepared by microwave heating and structural and fluorescence properties were studied. The crystal fluorescence of doped system is compared with solution fluorescence where both components are present in solvent. In order to obtain optical parameters of doped system required during fluorescence measurement, the optical

parameters for both donor and acceptor components were estimated from absorption, excitation and fluorescence spectra of individual components.

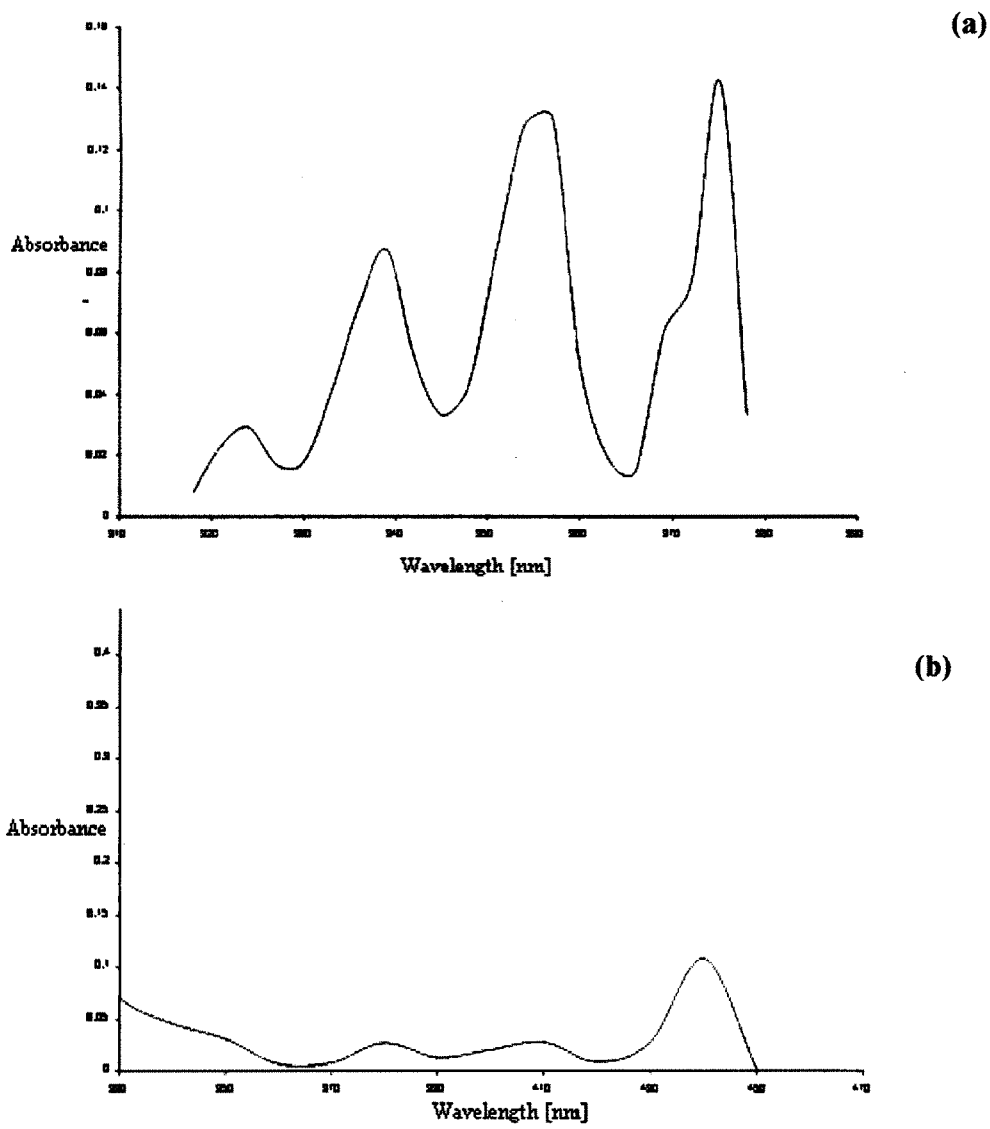

Fig. 3.16 Absorbance spectra of anthracene (a) and tetracene (b) in solution.

Fig. 3.16 shows absorption spectra of anthracene (a) and tetracene (b) in solution. It is seen that though the spectra of both components are structured the region of their occurrence are widely separated. The absorption region of anthracene is 320 nm to 380 nm while that of tetracene is 370 nm to 450 nm. The absorption spectra and excitation spectra are identical; both are linear planer molecules and belong to lattice 'A' type.

Fig. 3.17 illustrates excitation spectra of anthracene (1) and tetracene (2) in solution. The spectra are sharp, structured and seen widely separated as per expectation.

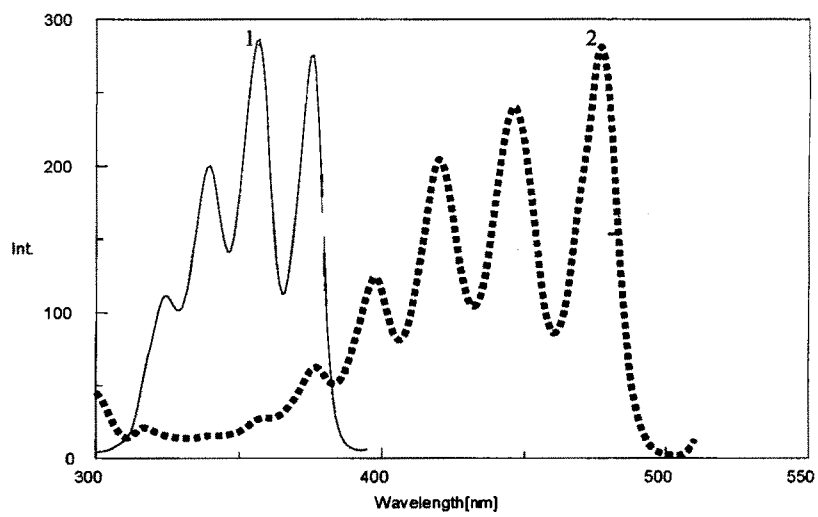

Fig 3.17 Excitation spectra of anthracene (1) and tetracene (2) in solution.

The excitation spectrum of anthracene occurs in 300 nm to 380 nm while intense band of tetracene are observed in the region 380 nm to 500 nm with maximum at 477 nm. The excitation maximum noted for anthracene is 356 nm. At this wavelength tetracene has negligible absorption.

The fluorescence spectrum of crystalline anthracene (1) shown in Fig. 3.18 occurs in the region where excitation of tetracene appears. This observation clearly indicates the probability of energetic interactions between anthracene and tetracene when approaches close enough. Figure also shows sufficient overlap between fluorescence of crystalline anthracene and excitation spectrum of tetracene to satisfy the criterion required for efficient EET to occur [83]. In addition to this singlet excited energy level of tetracene is lower lying than that of anthracene.

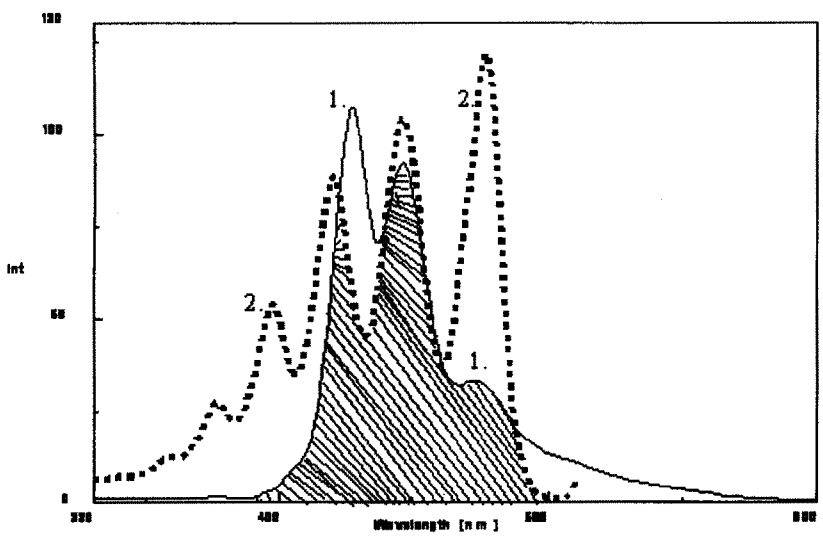

Fig.3.18 Fluorescence spectrum of crystalline anthracene (1) and excitation spectrum of tetracene in solution (2).

The efficiency of excitation energy transfer also depends upon the critical energy transfer distance (Ro) between donor and acceptor molecules. The value of Ro was estimated for present system by using Forster relation [18] as mentioned on page no.60. The estimated value of Ro is 44.6 A°. The values below 50 A° favor efficient energy transfer. Hence in the present studies anthracene doped by varying amounts of tetracene were prepared.

Fig. 3.19 shows fluorescence spectra of bare anthracene (1) and tetracene doped polycrystalline anthracene powders (2). The careful observation of spectra reveals that the incorporation of tetracene in the anthracene lattice introduces two changes. First the monomer, structured fluorescence of crystalline anthracene is quenched and second new structured emission appears in the region 460 nm to 600 nm. The red shifted emission is attributed to tetracene monomer emission [84]. The tetracene impurity changes blue fluorescence of anthracene into green. Thus addition of small amounts of tetracene into anthracene quenches the anthracene fluorescence and yields intense fluorescence of tetracene. This shows that there is efficient transfer of electronic excitation energy from

BARR. BALASAHEB KHARDEKAR LIBRARY
SHIVAJI UNIVERSITY, KOLHAPUR.

anthracene to tetracene. The energy transfer can occur radiatively or by a radiationless process which is a subject of experimental and theoretical studies. The mechanism by which energy transfer and emission occurs can be understand better by the emission studies performed as a function of tetracene concentration.

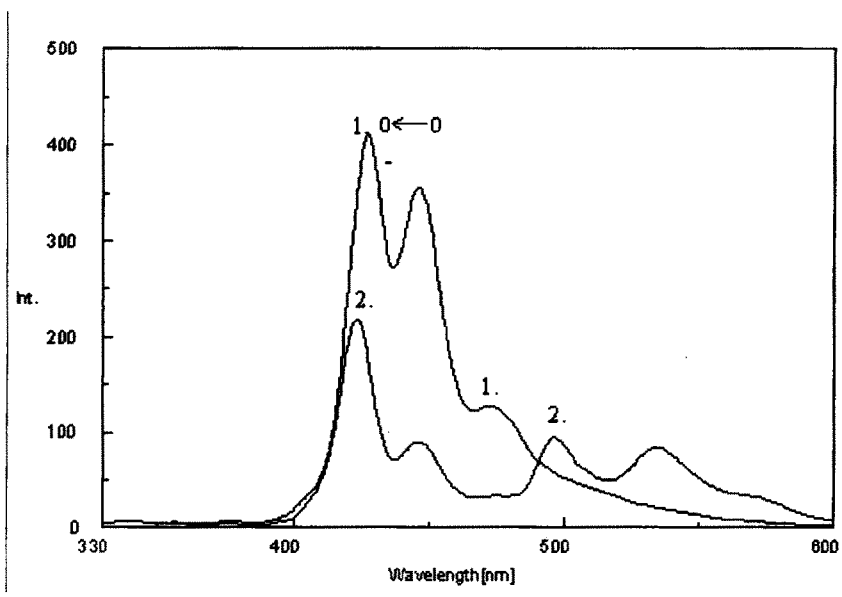

Fig. 3.19 Fluorescence spectra of pure crystalline anthracene (1) and 5x10^{-2} mole tetracene per mole anthracene (2).

Fig. 3.20 shows fluorescence spectra of anthracene doped by varying concentrations of tetracene monitored at λ_{ex} = 477 nm. The addition of tetracene in anthracene decreases the intensity of 0←0 band at 415 nm of anthracene and simultaneously the tetracene emission appears with its 0←0 band peaking at 500 nm. The spectral parameters such as intensity of 0←0 band of anthracene and tetracene, the spectral position of bands and relative ratio of intensity of acceptor (tetracene) to donor (anthracene) are given in the Table No.7.

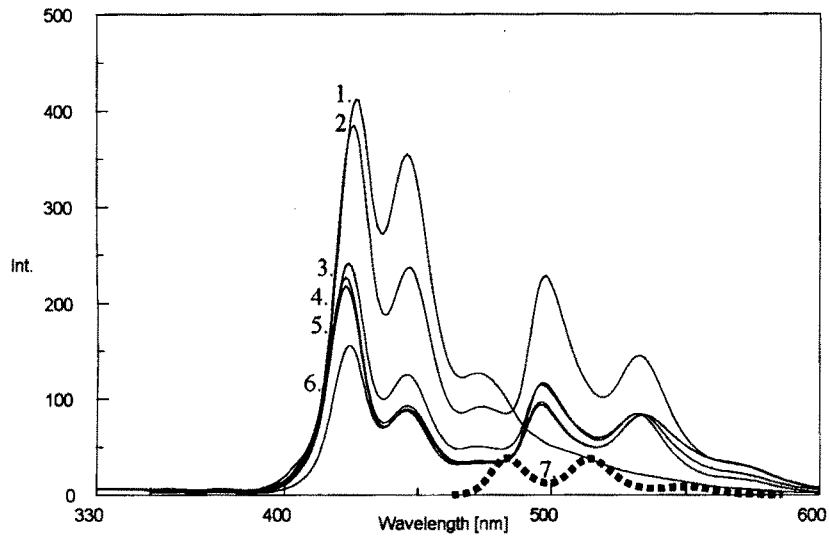

Fig. 3.20 Fluorescence spectra of tetracene doped anthracene in crystalline state; (1) Pure anthracene (2) $5x10^{-3}$ mole (3) $1x10^{-2}$ mole (4) $3x10^{-2}$ mole (5) $5x10^{-2}$ mole (6) $1x10^{-1}$mole of tetracene per mole anthracene and (7) Pure tetracene.

Table No. 7:-Spectral parameters of Anthracene doped tetracene luminophors

Sr. No.	Concentration of tetracene per mole of Anthracene	Monomer Fluorescence (donor)		Monomer Fluorescence (acceptor)		F_D/F_A
		λ_M	F_D	λ_M	F_A	
1	0	425	392.366	-	-	-
2	$5x10^{-3}$	425	382.027	497	228.003	1.6755
3	$1x10^{-2}$	425	266.422	497	117.69	2.2637
5	$3x10^{-2}$	425	239.45	497	114.921	2.0836
6	$5x10^{-2}$	425	208.419	497	93.449	2.2302
7	$1x10^{-1}$	425	155.578	497	117.134	1.3282

It is seen that concentration of tetracene does not introduces spectral changes in anthracene emission.

Mechanism

An excited host molecule interacts with its neighbors, leading to a rapid migration of the electronic excitation energy (exciton) through the crystal lattice. The magnitude of the exciton-phonon scattering due to interaction with the lattice vibrations determines the nature of the exciton migration. If the scattering is small as in pure crystal, the mean free

path of the coherent exciton wave is much larger than the lattice spacing (d). The exciton is delocalized over the whole crystal. In real crystal scattering is large, the exciton motion is in incoherent and described by the exciton trapping model. The exciton corresponds at any instants to the localized molecular state of excited host and the exciton migration is a random walk process in which the excitation energy hoops between neighboring molecules. In a mixed crystal when excited anthracene approaches sufficiently close to tetracene molecule and interact strongly with the neighboring anthracene molecule and energy transfer occurs. The probable processes are summarized below:

Presentation	**Process**	**Rate**
$A_{So} + h\nu \rightarrow [A_{S1}]^*$	Excitation	Ia
$[A_{S1}]^* \rightarrow A_{So}$ + heat	IC	$k_{ic}\,[A_{S1}]^*$
$[A_{S1}]^* \rightarrow [A_{T1}]^*$+ heat	ISC	$k_{isc}\,[A_{S1}]^*$
$[A_{S1}]^* \rightarrow A_{So} + h\nu_{fA}$	Donor fluorescence	$K_{fA}\,[A_{S1}]^*$
$[A_{S1}]^* + T_{So} \rightarrow A_{So} + T_{S1}^*$	EET	$k_{et}[A_{S1}]^*\,[T_{So}]$
$[T_{S1}]^* \rightarrow T_{So} + h\nu_{fT}$	Acceptor fluorescence	$k_{fl}[T_{S1}]^*$

[A] And [T] stands for Anthracene and Tetracene molecules respectively.

$$Ia = [k_{ic} + ki_{sc} + k_f][A_{S1}]^* \qquad \text{----------} \qquad (1)$$

$$[A_{S1}]^* = \frac{Ia}{k_{ic} + k_{isc} + k_{fA}} \qquad \text{----------} \qquad (2)$$

Hence quantum yield of fluorescence ϕf_A in absence of acceptor is,

$$\Phi_{fA} = \frac{k_{fA}[S_1]}{Ia} = \frac{k_{fA}}{k_{ic} + k_{isc} + k_{fA}} \qquad \text{----------} \qquad (3)$$

Similarly for $[T_{S1}]^*$,

$$k_{et}[A_{S1}]^*[T_{SO}] = k_{fT}[T_{S1}]^* \quad \text{----------} \quad (4)$$

$$\therefore [T_{S1}]^* = \frac{k_{et}[A_{S1}]^*[T_{SO}]}{k_{fT}} \quad \text{----------} \quad (5)$$

$$[TS1]^* = \frac{k_{et} \cdot Ia}{k_{ic} + k_{isc} + k_{fA}} \cdot \frac{[T_{SO}]}{k_{fT}} \quad \text{----------} \quad (6)$$

$$[T_{S1}]^* = \frac{Ia}{k_{fT}}\left[\frac{k_{et}}{k_{ic} + k_{isc} + k_{fA}}\right][T_{SO}] \quad \text{----------} \quad (7)$$

$$\Phi_{fT} = \frac{Ia \cdot k_{fT}}{k_{fT} \cdot Ia}\left[\frac{k_{et}}{k_{ic} + k_{isc} + k_{fA}}\right] \cdot [T_{SO}] \quad \text{----------} \quad (8)$$

$$\Phi_{fT} = \left[\frac{k_{et}}{k_{isc} + k_{ic} + k_{fA}}\right] \cdot [T_{SO}] \quad \text{----------} \quad (9)$$

$$\left[\frac{\Phi_{fA}}{\Phi_{fT}}\right] = \left[\frac{k_{fA}}{k_{ic} + k_{isc} + k_{fA}}\right] \cdot \left[\frac{k_{isc} + k_{ic} + k_{fA}}{k_{et}}\right] \cdot \left[\frac{1}{T_{SO}}\right] \quad \text{----------} \quad (10)$$

$$\frac{\Phi_{fT}}{\Phi_{fA}} = \left[\frac{k_{ic} + k_{isc} + k_{fA}}{k_{fA}}\right] \cdot \left[\frac{k_{et}}{k_{ic} + k_{isc} + k_{fA}}\right] \cdot [T_{SO}] \quad \text{----------} \quad (11)$$

$$\left[\frac{\Phi_{fT}}{\Phi_{fA}}\right] = \left[\frac{k_{et}}{k_{fA}}\right] \cdot [T_{SO}] \quad \text{----------} \quad (12)$$

$$\left[\frac{\Phi_{fT}}{\Phi_{fA}}\right] = \pi o \cdot k_{et} \cdot [T_{SO}] \quad \text{----------} \quad (13)$$

Quantum efficiency is obtained from the area under curve or from the intensity of emission at the wavelength of maximum emission.

$$\therefore \left[\frac{F_T}{F_A}\right] = \tau o \cdot k_{et} \cdot [T_{SO}] \qquad \text{----------} \qquad (14)$$

$$Slope = \tau o \cdot k_{et} \qquad \text{----------} \qquad (15)$$

$$k_{et} = \frac{slope}{\tau o} \qquad \text{----------} \qquad (16)$$

$$\boxed{\therefore k_{et} = 1 \text{ x } 10^9 \text{ sec.}}$$

The validity of equation (14) is tested experimentally by plotting F_T/F_A Vs [TSo] as shown in Fig. 3.21. The figure shows the straight line with coefficient of linear regression (R^2) 0.8248. The value of R^2 close to one indicates validity of equation and therefore the quenching of anthracene fluorescence and sensitization of tetracene fluorescence is occurring as per the proposed mechanism. In addition to this quenching of anthracene fluorescence by tetracene is obeying the Stern-Volmer relation also. Fig. 3.22 plot of Fo/F Vs [TSo] is straight line with intercept one. The quenching rate constant is 4.19×10^9 sec. The rate constant for energy transfer estimated from equation (16) is 1×10^9 sec^{-1}. Thus doping of tetracene in anthracene favors efficient EET than in solution due to closer approach of molecules in the lattice of anthracene host.

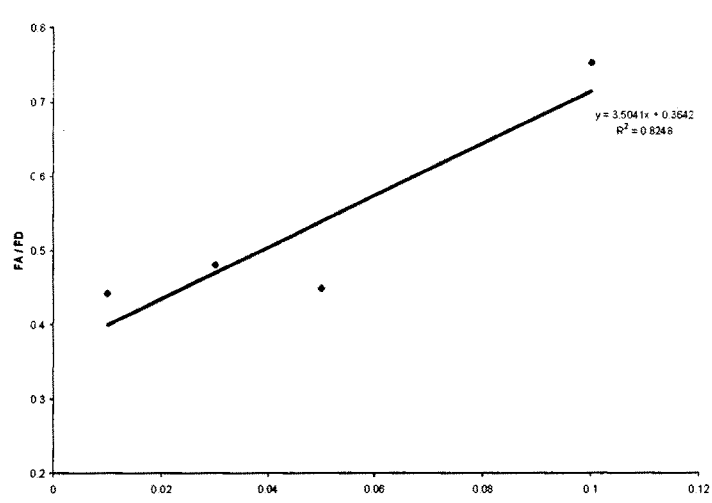

Fig. 3.21 a plot of F_T / F_A Vs concentration of tetracene.

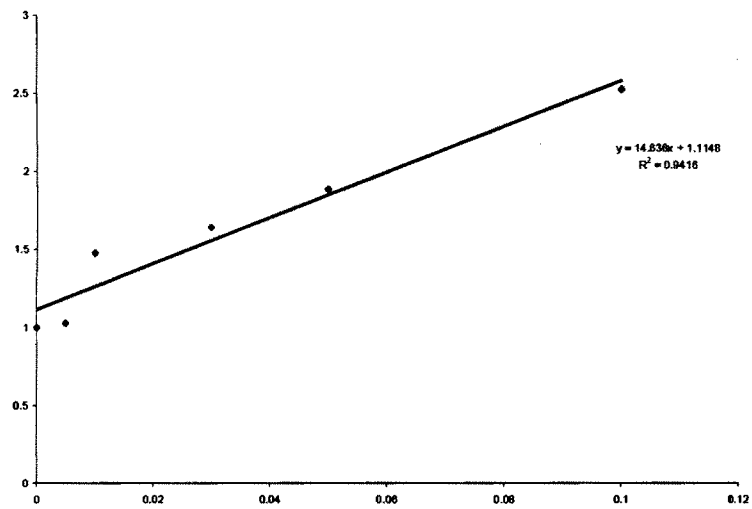

Fig. 3.22 Stern-Volmer plot.

3.6.2.1 Structural properties

Anthracene and tetracene form series of solid solutions. The X-ray diffraction profile of pure as well as tetracene doped anthracene is given in Fig.3.23. The crystalline nature of sample is confirmed as peaks obtained are sharp and well defined. The XRD profile of anthracene is used as fingerprint and is compared with spectra of doped one. From figure it is observed that there is only slight change in peak positions (2θ values). No additional peaks are observed in XRD profile of doped samples. There is only increase in intensity indicating formation of homogeneous mixed crystals. The intense band [001] was broadened using band broaden technique and used to calculate grain size of doped anthracene samples using Scherer formula [71]. It is also observed that doping a pure crystal with impurity creates deformation in crystal which otherwise changes microstain, dislocation density and stacking fault which are tabulated in Table No.8.

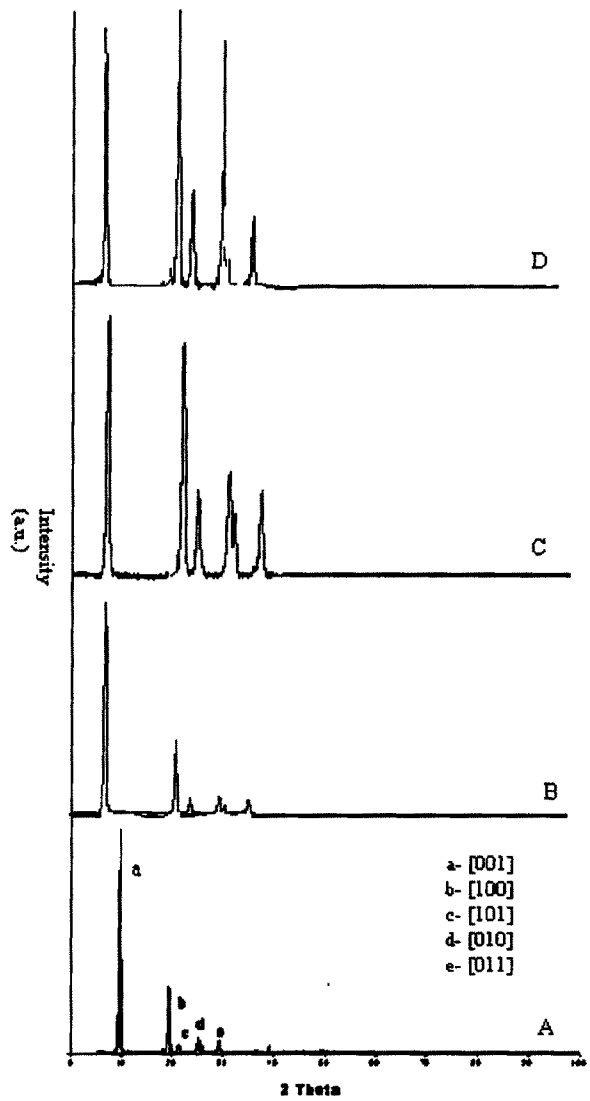

Fig.3.23 Powder X-ray diffraction profile of anthracene and tetracene doped anthracene; (A) Pure anthracene (B) $5x10^{-3}$, (C) $1X10^{-2}$ and (D) $1X10^{-1}$ mole of tetracene per mole anthracene.

From table it is observed that values of grain size go on decreasing with addition of tetracene which may be because of formation of newer smaller grains over larger grains. On the other hand values of microstain, dislocation density and stacking fault goes on decreasing with increase in concentration of tetracene indicating deformation of host crystal. The careful observation shows that for lower concentration of tetracene the anthracene is not much deformed. However, at higher concentration e.g. at 1×10^{-1} mole

of tetracene per mole of anthracene, host crystal is deformed as values of microstain and stacking fault are seen to be decreased appreciably.

Table No. 8:- Structural parameters of anthracene doped tetracene luminophors

Concentration Moles of tetracene per mole anthracene	Glancing angle (2θ) degree	FWHM $\beta_{2\theta}$	Microstain $\varepsilon \times 10^{-3}$ l^2/m^{-4}	Dislocation density $\rho \times 10^{15} cm^{-2}$	Grain size (D) A^O	Stacking fault α_{st}
0	9.702	0.345	1.71	1.51	201.4	0.2995
$5x10^{-3}$	9.562	0.340	1.69	1.44	204.5	0.2974
$1x10^{-2}$	9.433	0.328	1.63	1.37	212.0	0.2889
$1x10^{-1}$	9.536	0.317	1.57	1.25	219.3	0.2777

3.6.3 9-Vinylanthracene doped anthracene luminophors

3.6.3.1 Optical Properties

The excitation (a) and fluorescence (b) spectra of crystalline anthracene presented in Fig.3.24, exhibit mirror image relationship and are largely Stoke shifted. The observed Stoke shift is because of intermolecular forces of attraction between neighboring anthracene molecule in its herringbone structure proposed by Garezzotti et al. [85]. The structured fluorescence of anthracene shows two clearly resolved peaks with shoulder on low energy side. The location of the band maxima for three components of $1L_a$ transition of anthracene is assigned as 0←0; 0←1 and 0←2. The first band corresponding to 0←0 transition is more intense and wavelength of maximum emission band corresponding to this transition is 427 nm. This band is Stoke shifted from 0←0 vibronic band in excitation spectrum by 997 cm^{-1}. The fluorescence spectrum of anthracene doped by VA is also shown in the same Fig.3.24 (spectrum-c). The careful comparison of this spectrum with the spectrum of bare anthracene reveals that the incorporation of VA does not change the spectral region of anthracene but the vibronic band intensities seen to be changed. The high energy band corresponding to 0←0 transition is quenched and nearby 0←1 is enhanced. These vibronic changes induced in excited anthracene molecule by VA exhibits shift in λ_{em} from 427 nm to 446 nm. The fluorescence of VA expected to occur in the region 400-500 nm is not observed [86].

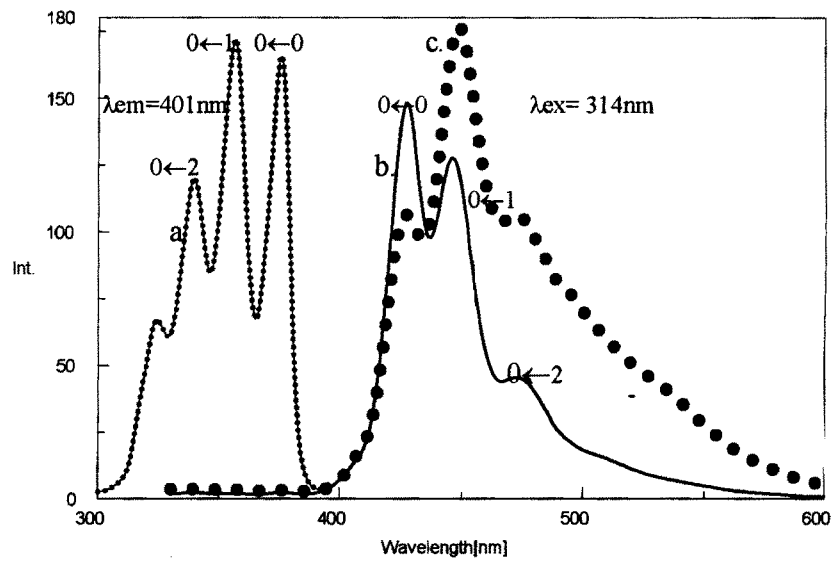

Fig. 3.24 Normalized excitation (a); fluorescence spectra of pure anthracene (b); and anthracene doped by $3x10^{-2}$ mole VA (c).

This conclusion is further supported by the fact that the excitation spectrum of VA (2) shown in Fig.3.25 is widely separated from the fluorescence spectrum of the crystalline anthracene (1). Hence it is believed that the observed anthracene spectral changes in terms of vibronic band intensity in anthracene are because of polar VA dopant.

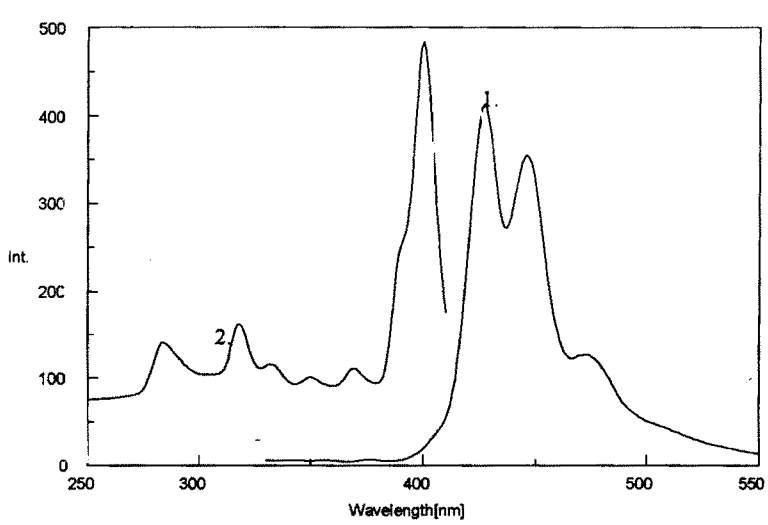

Fig. 3.25 Spectral separation between fluorescence spectrum of anthracene (1) and excitation spectrum of VA (2).

The evolution of fluorescence features of anthracene was studied as a function of concentration of VA. Fig. 3.26 shows the fluorescence spectra with various concentration of VA as impurity in anthracene host at room temperature. It is evident from the figure that no energy shifts are observed for any of the three peaks when concentration is increased. It is seen that as concentration of VA increases the intensity of both vibronic bands decreases. The rate of decrease in intensity of 0←0 band is more and hence at and above 1 x 10^{-2} mole dopant concentration actually its intensity becomes less than that of 0←1 band. The spectral shape of anthracene containing high dopant concentration seems to be reversed when compared to spectrum of undoped anthracene (Fig.3.24).

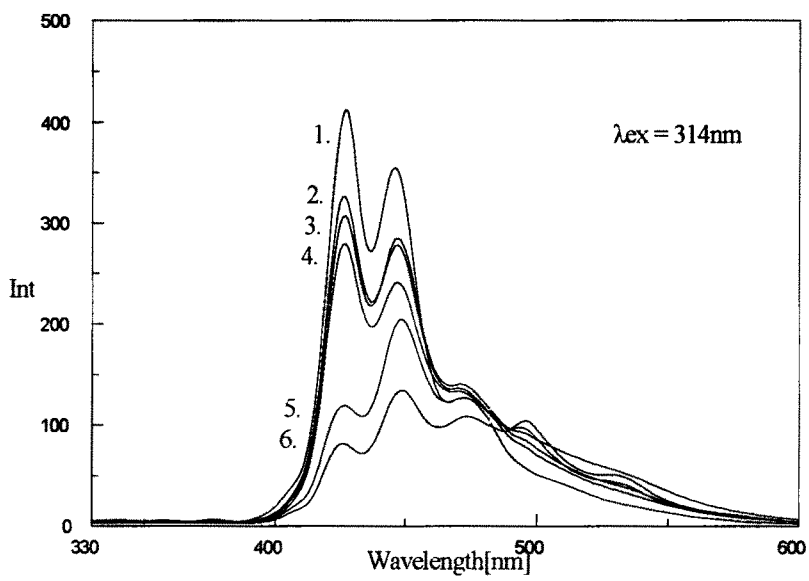

Fig. 3.26 Fluorescence spectra of anthracene doped by VA; (1) Pure anthracene (2) 1x10^{-3} mole; (3) 5x10^{-3} mole; (4) 1x10^{-2} mole; (5) 3x10^{-2} mole; and (6) 5x10^{-2} mole of VA per mole anthracene.

The ratio of fluorescence intensity of the bands ($F_{0\leftarrow1}$ to $F_{0\leftarrow0}$) is determined and plotted against the dopant concentration. The nature of plot presented in Fig.3.27 indicates that the ratio $F_{0\leftarrow1}$/ $F_{0\leftarrow0}$ increases with the doping concentration, reaches to maximum at 3 x 10^{-2} mole of VA per mole anthracene. The broad, structure less excimer fluorescence of VA expected with λ_{em}= 515 nm is not seen even at higher dopant concentration. This observation rules out possibility of induced excitation by EET from excited anthracene to VA molecule.

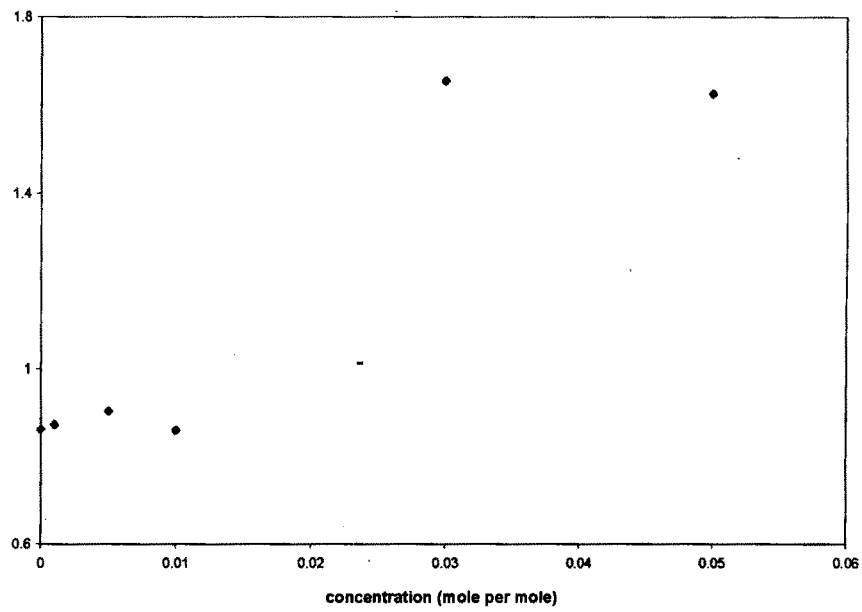

Fig.3.27 Variation of relative ratio of vibronic band intensities ($f_{0\leftarrow1}/f_{0\leftarrow0}$) in fluorescence as a function of concentration of VA (mole per mole).

The dopants can be classified into three types. Some are inert, only quenches host fluorescence by collisional quenching, some change the host emission lines and some give guest fluorescence due to excitation energy transfer (EET). The observed results indicate the effect of dopant concentration in term of changes in the intensities of emission lines of anthracene. The band intensities are related with oscillatory transition strength (f) which is proportional to the integrated area of the fluorescence peak of the band [87]. The estimated values are listed in Table. No.9. In addition to this the full width at half maximum (FWHM) is also noted and given in the same table. The dependence of the relative oscillatory strength of the transition bands of anthracene as function of VA concentration are illustrated in Fig.3.28. These plots are linear and nature is descending for 0←0 bands while ascending for 0←1 band. The plot fits into linear regression equation with correlation coefficient $R^2 = 0.9536$ and $R^2 = 0.9184$ for low energy and high energy band respectively.

Table No. 9:- Summary of vibronic band intensities and relative oscillatory strength (f) in anthracene doped by various amount of VA

Concentration of VA (per mole of anthracene)	Emission band intensity (a.u.) for transitions at		FWHM (nm)		Relative Oscillatory Strength f (a.u.)	
	427nm 0←0	446nm 0←1	0←0	0←1	0←0	0←1
0	412.297	352.770	12.02	12.05	1.0000	1.0000
1×10^{-3}	325.744	284.879	12.49	12.46	0.8173	1.1749
5×10^{-3}	307.178	278.600	12.30	12.66	0.7694	1.1908
1×10^{-2}	279.792	241.312	12.55	12.38	0.7038	1.3180
3×10^{-2}	119.423	203.325	11.22	13.24	0.3384	1.5879
5×10^{-2}	81.366	132.302	10.88	12.89	0.2305	2.3346

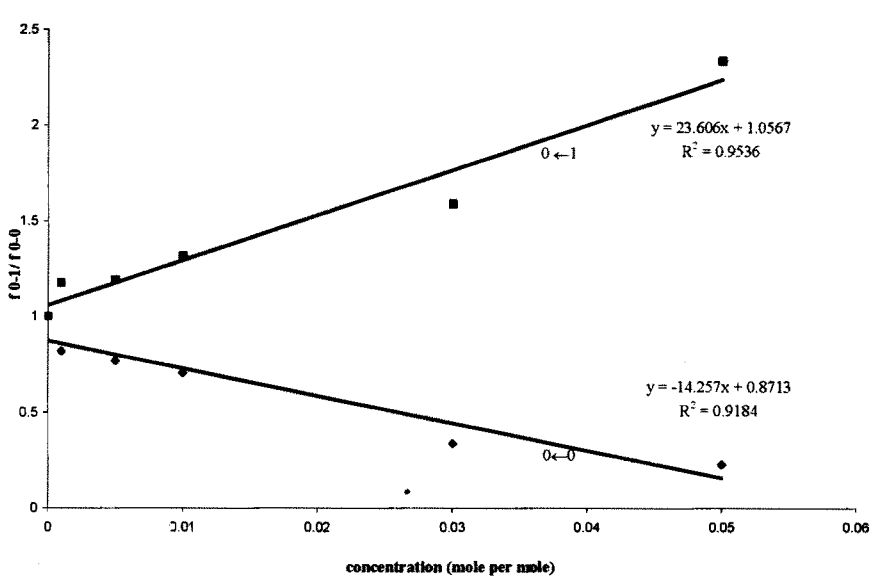

Fig.3.28 Relative oscillatory transition strength of vibronic bands in (0←0) and (0←1) in fluorescence of anthracene as a function of VA concentration (mole per mole).

The results indicate that transition probability of 0←0 band decreases while at the same time that of 0←1 increases by the same amount as correlation coefficients are nearly identical. The FWHM of 0←0 bands seems to decrease while that of 0←1 band

remains nearly constant ≈ 12 nm. The spectral band width at half maximum less than 15 nm indicates saturated color emission. The typical molecular organic light emitting diodes (LEDs) have FWHM of between 60 to 100 nm and for some polymers and phosphorescent molecule it has shown to be as narrow as 26 nm [88]. The doped anthracene system has exhibited vibronic emission lines of much narrow band width. The lower dopant concentration does not induce significant changes in the relative oscillatory strength of 0←0 and 0←1 transition and the values are not much different However, at higher dopant concentration oscillatory strength of 0←1 band is about 5 to 10 times greater than that of 0←0 band. The observed results led us to conclude that the increase in relative oscillatory strength of the vibrational states of excited manifold of anthracene is because of the presence of the VA only which interacts with excited anthracene and altering its electronic configuration. The polar dopant effect on change in structure of anthracene emission is further confirmed by similar studies performed on the MA doped anthracene and CA doped anthracene. The spectral results illustrated in the Fig. 3.29, indicate the quenching of 0←0 bands and sensitization of 0←1 band.

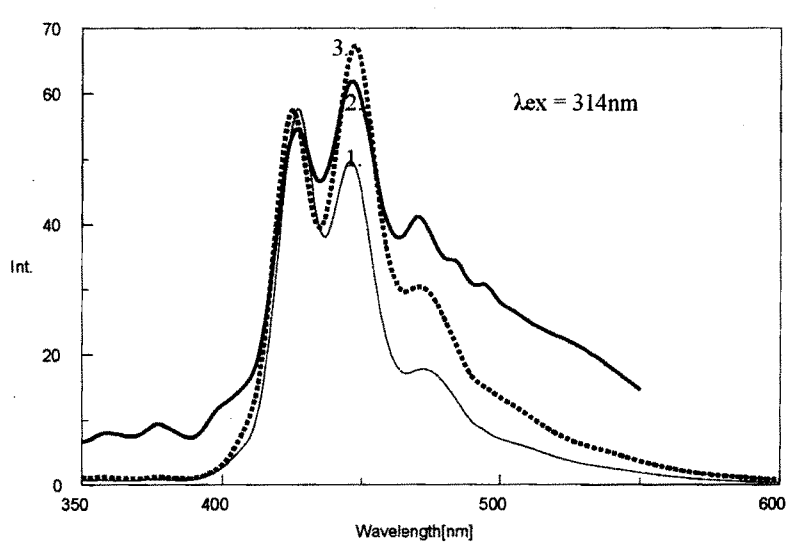

Fig. 3.29 Normalized fluorescence spectra of crystalline powders of (1) Pure anthracene (2) anthracene doped by MA and (3) anthracene doped by CA.

Possible mechanism of spectral changes

Anthracene doped tetracene is classic system where very efficient transfer of singlet energy occurs. The blue anthracene fluorescence is quenched and characteristic green fluorescence of tetracene in this system was shown to appear because of anthracene exciton (excited electron-hole pair) trapped at physical defect created by tetracene in doped lattice [89]. However every doping does not induce traps. In the present study, characteristic VA fluorescence is not observed upon optical excitation of doped anthracene as in tetracene doped anthracene system. The doped crystals behaved just as expected. The quenching in doped anthracene containing small amount of VA is because of migration of excitation energy (exciton) in random fashion through the lattice and will remain with foreign VA molecule until dissipated non-radiatively. However concentration of dopant does not quench the anthracene fluorescence appreciably, rather sensitize low energy vibronic band as compared to high energy band. These induced spectral changes modify sh[redacted]f anthracene spectrum and wavelength of maximum emission appears to be shifted. Compared to tetracene or other similar type of dopant (perylene, pentacene) VA is polar and thought to act in different manner. The solid state solvation effect reported in literature indicates that the closely packed polar solute in the organic molecular solids induce appreciable red spectral shift in the emission spectrum by local electric field [90]. The solid state solvation (SSS) luminescence is explained on the basis of energy structures both for excitons and for conduction level. On the basis of available information we have proposed energy level diagram for anthracene as shown in Fig 3.30. The excitation and fluorescence spectra of anthracene indicate that the transition corresponds to different vibronic states in singlet S_1 band labeled as S_1 (0←Vn). Using this conventional scheme the transition are labeled as S_1 (0←0), S_1 (0←1), and S_1 (0←2). The excited anthracene molecule is expected to be more polarizable as electron in the excited state occupies a more extended orbital than in the ground state. The presence of larger amounts of VA in the anthracene lattice generate strong local electric field which is acting across the excited anthracene molecule and induce changes both in the molecular vibrational energy levels and transition dipoles leading to Stark effect [91]. These effects results into the increase in overlap of S_0 ground state wave function with S_1 vibronic levels thereby favoring the transition to higher vibrational levels [92]. The observed

relative oscillatory strength of S_1 (0←1) is more than that of S_1 (0←0) in even for lower for lower concentration of VA and becomes more than ten times for higher concentration. Therefore, with increase in VA concentration the transition to the higher vibrational levels are expected to increase faster than that of lower Vibrational levels of S_0 states, from zeroth vibrational level of excited singlet S_1. The 0←1 transition bands become more prominent than 0←0 at higher VA in anthracene lattice and λ_{em} seem to be spectrally shifted.

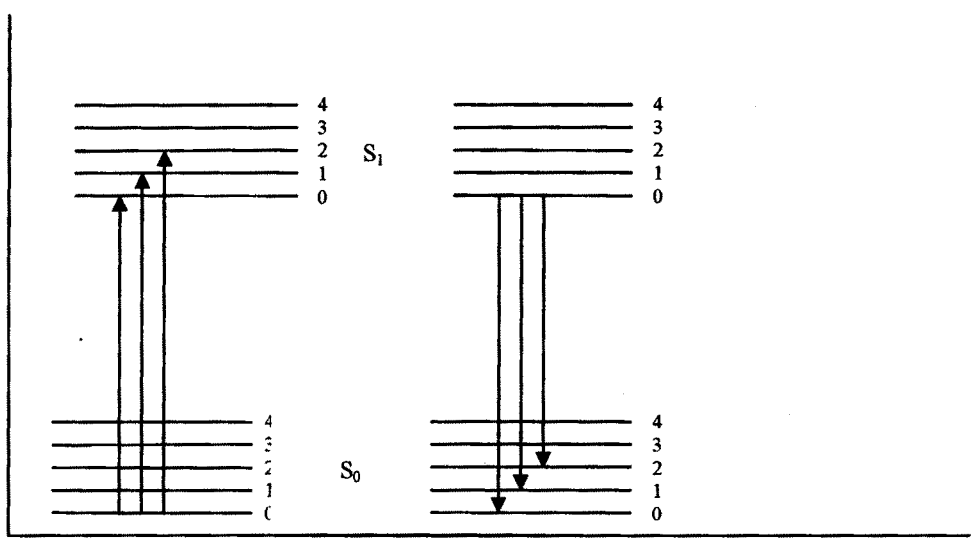

Fig. 3.30 Energy level diagram for anthracene.

3.6.3.2 Structural Properties

Series of solid solutions are formed by anthracene and VA. The X-ray diffraction pattern of doped anthracene crystals along with its pure one is represented in Fig. 3.31. Here also peaks are sharp and well defined. No additional lines are seen in spectra of doped luminophors when compared with that of pure anthracene indicating formation of homogeneous mixed crystals. The intense band was indexed and used to calculate grain size and other parameters such as microstain, dislocation density and stacking fault.

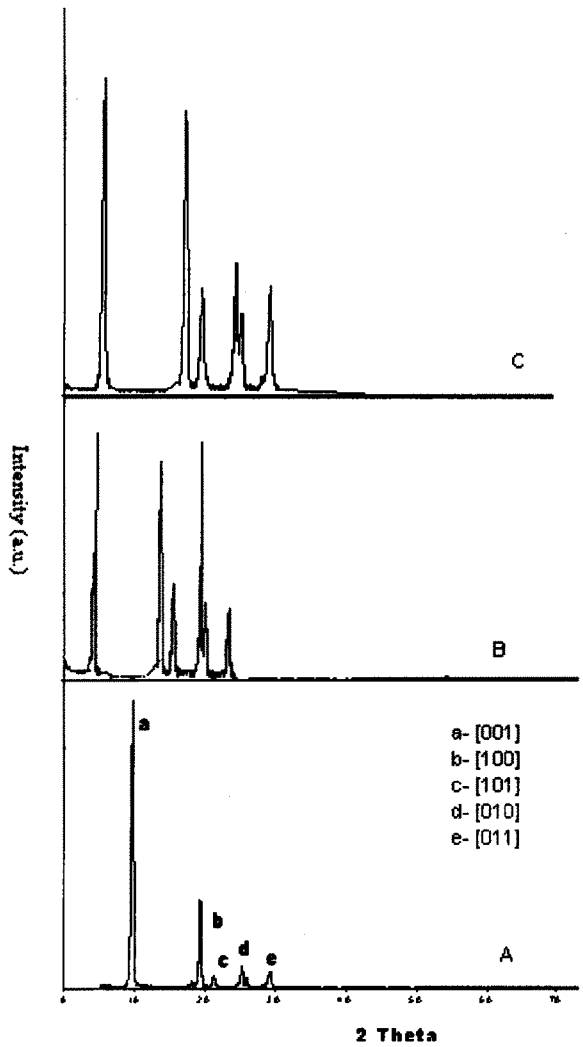

Fig.3.31 Powder X-ray diffraction profile anthracene and 9-vinylanthracene doped anthracene. (A) Pure anthracene (B) $5x10^{-3}$ and (C) $1x10^{-2}$ mole 9-vinylanthracene per mole anthracene.

The values tabulated in Table No. 9 indicate decrease in grain size as concentration of VA increases indicating formation of newer smaller grains on larger one. Due to deformation in host crystal other parameters goes on decreasing with increase in concentration of VA. The careful observation shows that for lower concentration of VA the anthracene is not much deformed. However, at higher concentration e.g. at 1 x 10^{-1}

mole of VA per mole of anthracene, host crystal is deformed as values of microstain and stacking fault are seen to be decreased appreciably.

Table No. 9:- Structural parameters of Anthracene doped 9-vinylanthracene (9-VA) luminophors

Concentration Moles of 9-VA per mole anthracene	Glancing angle (2θ) degree	FWHM $\beta_{2\theta}$	Microstain $\varepsilon \times 10^{-3}$ l^2/m^{-4}	Dislocation density $\rho \times 10^{15} cm^{-2}$	Grain size (D) A^O	Stacking fault α_{st}
0	9.702	0.345	1.71	1.51	201.4	0.2995
$3x10^{-2}$	9.572	0.358	1.78	1.60	194.3	0.3130
$5x10^{-2}$	9.659	0.344	1.71	1.48	202.1	0.2994
$1x10^{-1}$	9.707	0.308	1.53	1.18	225.8	0.2674

3.6.4 9-Chloroanthracene doped anthracene luminophors

3.6.4.1 Optical Properties

9-Chloroanthracene and 9-vinylanthracene are both substituted anthracene and in our initial studies it is observed that their fluorescence spectra in dilute solution are sharp and structured like the parent anthracene. The substitution at 9-position only shifted the wavelength of maximum emission (λ_{em}) towards red when compared with λ_{em} of anthracene solution. The fluorescence spectra of crystalline VA and CA exhibits excimer fluorescence and both belong to lattice 'D' type where lateral π-orbital overlap between adjacent molecules is larger. The results of spectral shift obtained for doped anthracene crystalline powders are explained on the basis of solid state solvation effect exhibited by VA. To confirmed and support this effect a dopant of similar nature CA was tested and optical properties are measured for various luminophors of crystalline anthracene doped by CA. The fluorescence studies are performed as in previous system and results are interpreted in the light of solid state solvation effect.

Fig. 3.32 shows fluorescence spectrum of anthracene (1) and excitation spectrum of CA (2). The spectral separation seen in the fig. 3.25 indicates that the excitation energy transfer from excited anthracene molecule to ground state CA molecule is improbable. However inspite of EET, the anthracene doped by CA has exhibited interesting results like the VA doped anthracene crystalline powder.

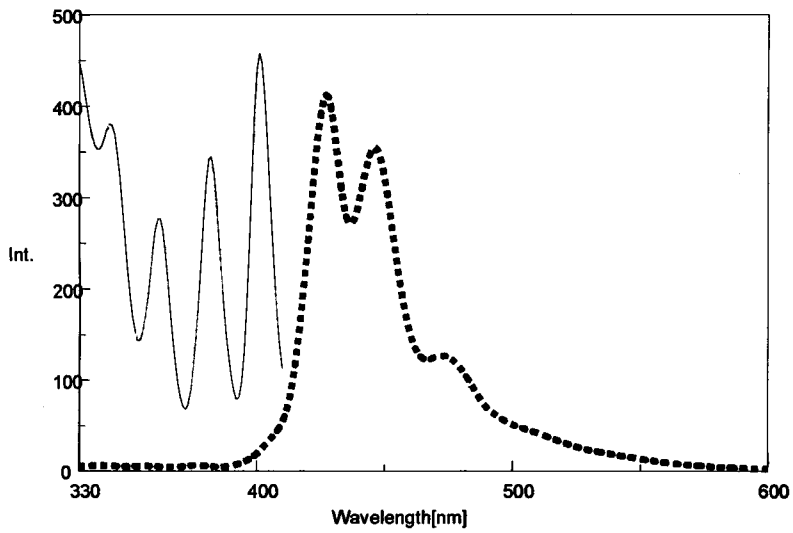

Fig. 3.32 Spectral separation between fluorescence spectrum of anthracene (1) and excitation spectrum of CA (2).

Fig.3.33 shows normalized excitation (A), fluorescence spectra (B) of pure anthracene and anthracene doped by 3 x 10^{-2} mole CA (C). The 0←0 fluorescence band of crystalline anthracene is seen to be suppressed and 0←1 band is enhanced in doped anthracene. The Stokes shift is changed from 0.002341 cm^{-1} to 0.002493 cm^{-1} by addition of dopant. The careful observation of fluorescence spectra of bare anthracene and doped anthracene reveal that the spectral shift towards red by about 1518 cm^{-1} and wavelength of maximum emission is changed from 401 nm to 427 nm.

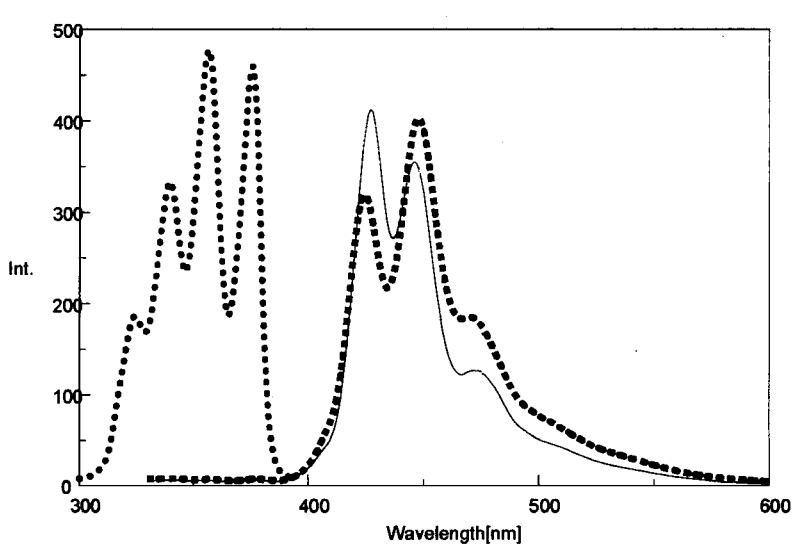

Fig. 3.33Normalized excitation (A), fluorescence spectra of pure anthracene (B), and anthracene doped by 3x10^{-2} mole CA (C).

The effect of dopant concentration on fluorescence spectrum of anthracene is shown in fig. 3.34. It is seen that the incorporation of CA decreases the intensity of both 0←0 as well as 0←1 vibronic emission bands but the rate of decrease in intensity seem to be different. The monomer fluorescence of CA expected to occur in range from 400 nm to 500 nm with maximum at 422 nm and shown in Fig.3.8 is not seen in the fluorescence spectrum of doped anthracene. Similarly excimer fluorescence of crystalline CA shown in the same Fig.3.8 is also not appeared. These observations rules out the possibility of formation of excited CA molecule by EET from anthracene molecule which could interact with its own ground state CA molecule and could emit excimer fluorescence. The spectral separation seen in fig.3.29 between emission of anthracene and excitation spectrum of CA has also indicated improbability of EET between host and dopant molecules. Hence it is believed that spectral changes observed in anthracene in terms of vibronic band intensities are due to polar CA dopant. The ratio of fluorescence intensity of the bands ($F_{0\leftarrow1}$ to $F_{0\leftarrow0}$) is determined and plotted against the concentration of chloroanthracene reaches to maximum for the doped anthracene containing 5 x 10^{-3} mole CA as shown in Fig.3.35. Thus the observed results indicate the effect of dopant concentration in terms of changes in the intensities of emission lines of anthracene.

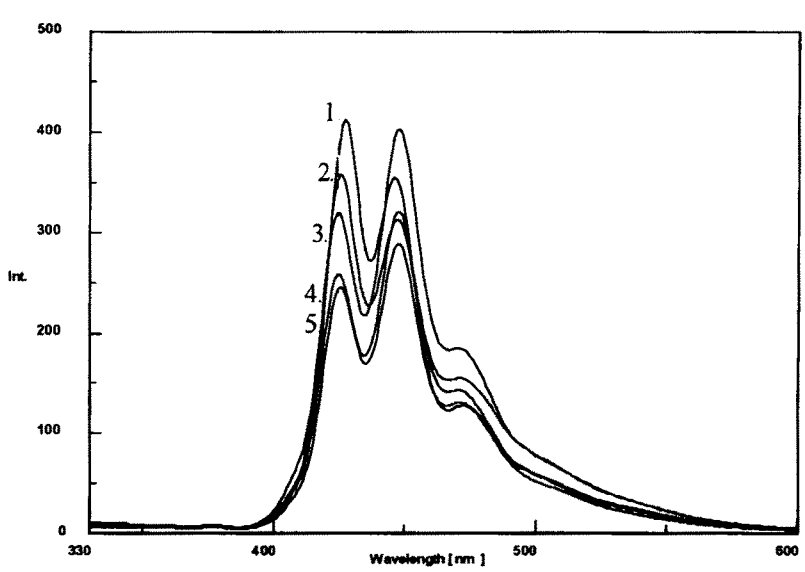

Fig 3.34 Fluorescence spectra of CA doped anthracene crystalline powders: 1) pure anthracene 2) 1x10^{-3} mole 3) 5x 10^{-3} mole 4) 1x10^{-2} mole and 5) 3x10^{-2} mole of CA per mole anthracene.

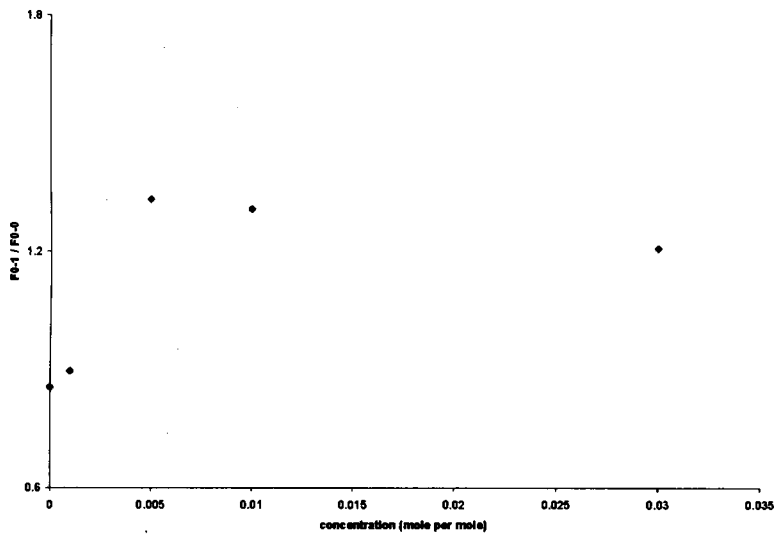

Fig. 3.35 Variation of relative ratio of vibronic band intensities ($F_{0\leftarrow1}$/ $F_{0\leftarrow0}$) in fluorescence as a function of concentration of CA (mole per mole).

The band intensities are related with oscillatory transition strength (*f*) which is proportional to the integrated area of the fluorescence peak of the band. The estimated values are listed in Table No. 9. In addition to this the full width at half maximum (FWHM) is also noted and given in the same table.

Table No. 10:- Summary of vibronic band intensities and relative oscillatory strength (f) in anthracene doped by various amount of CA

Concentration of CA (per mole of anthracene)	Emission band intensity (a.u.) for transitions at 427nm 0←0	447nm 0←1	FWHM (nm) 0←0	0←1	Relative Oscillatory Strength f (a.u.) 0←0	0←1
0	412.297	352.770	12.02	12.02	1.0000	1.0000
$1x\ 10^{-3}$	349.427	313.273	12.12	12.12	0.9011	1.0585
5×10^{-3}	301.78	401.991	11.63	11.63	0.8546	1.0647
1×10^{-2}	245.207	320.523	11.62	11.62	0.8010	1.0768
3×10^{-2}	238.432	287.968	11.73	11.73	0.6398	1.1973

The dependence of the relative oscillatory strength of the transition bands of anthracene as function of CA concentration are illustrated in Fig.3.36.

BARR. BALASAHEB KHARDEKAR LIBRARY
SHIVAJI UNIVERSITY, KOLHAPUR.

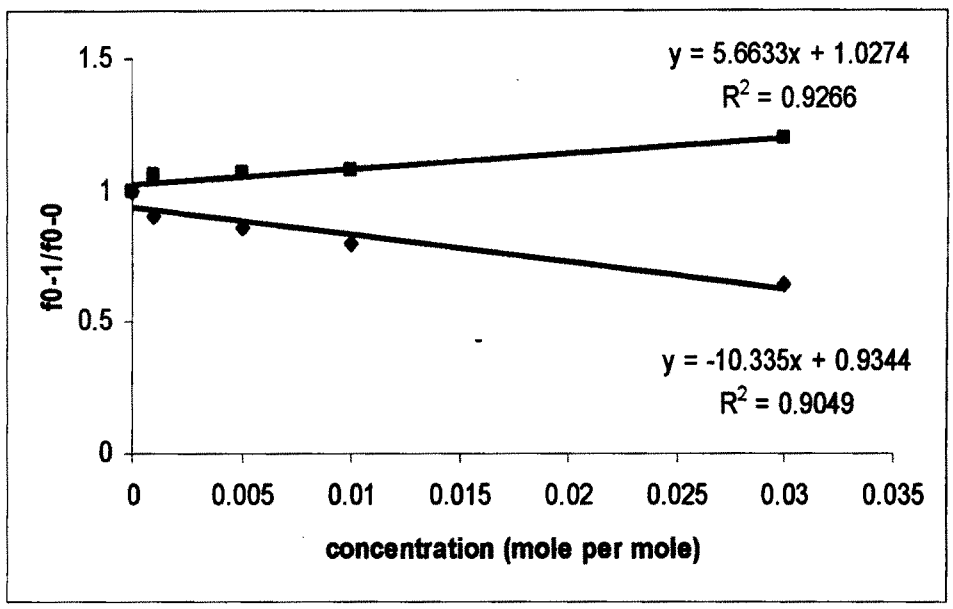

Fig. 3.36 Relative oscillatory transition strength of vibronic bands in (0←0) and (0←1) in fluorescence of anthracene as a function of CA concentration (mole per mole).

These plots are linear and nature is descending for 0←0 bands while ascending for 0←1 band. The plot fits into linear regression equation with correlation coefficient R^2 = 0.9266 and R^2 = 0.9049 for low energy and high energy band respectively. The results indicate that transition probability of 0←0 band decreases while at the same time that of 0←1 increases by the same amount as correlation coefficients are nearly identical. The FWHM of 0←0 bands seems to decrease while that of 0←1 band remains nearly constant ≈ 12 nm. The spectral band width at half maximum less than 5 nm indicates saturated color emission. The doped anthracene system has exhibited vibronic emission lines of much narrow band width. The lower dopant concentration does not induce significant changes in the relative oscillatory strength of 0←0 and 0←1 transition and the values are not much different However, at higher dopant concentration oscillatory strength of 0←1 band is about 5 to 10 times greater than that of 0←0 band. The observed results led us to conclude that the increase in relative oscillatory strength of the vibrational states of excited manifold of anthracene is because of the presence of the CA only which interacts

with excited anthracene and altering its electronic configuration.

3.6.4.2 Structural Properties

The X-ray diffraction profile of doped as well as undoped samples was presented in Fig. 3.37. The intense line was used to calculate grain size and other structural parameters which are tabulated in Table No.10. The careful observation shows that for lower concentration of VA the anthracene is not much deformed. However, at higher concentration e.g. at 1 x 10^{-1} mole of VA per mole of anthracene, host crystal is deformed as values of microstain and stacking fault are seen to be decreased appreciably.

Table No. 10:- Structural parameters of Anthracene doped 9-chloroanthracene (9-CA) luminophors

Concentration Moles of 9-CA per mole anthracene	Glancing angle (2θ) degree	FWHM $\beta_{2\theta}$	Microstain $\mathcal{E} \times 10^{-3}$ l^2/m^{-4}	Dislocation density $\rho \times 10^{15} cm^{-2}$	Grain size (D) A^O	Stacking fault α_{st}
0	9.702	0.345	1.71	1.51	201.4	0.2995
1 x 10^{-2}	9.618	0.375	1.86	1.75	185.5	0.3271
5x 10^{-2}	9.414	0.345	1.72	1.49	201.2	0.3041
1 x 10^{-1}	9.559	0.313	1.56	1.22	222.11	0.2738

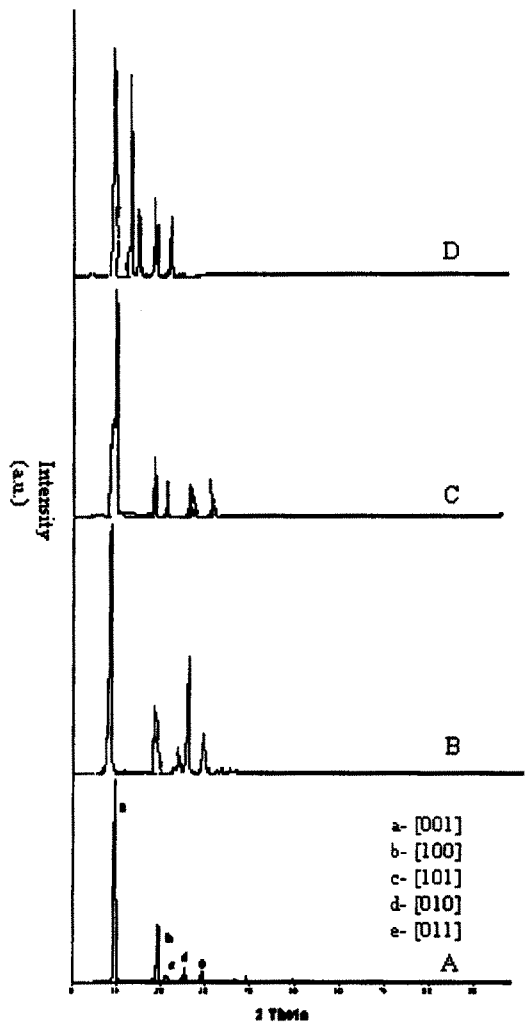

Fig.3.37 Powder X-ray diffraction profile of anthracene and 9-chloroanthracene doped anthracene; (A) Pure anthracene, (B) $1x10^{-3}$, (C) $1x10^{-2}$ and (D) $3x10^{-2}$ mole of 9-chloroanthracene per mole anthracene.